THE UNIVERSITY OF MICHIGAN
INDUSTRY PROGRAM OF THE COLLEGE OF ENGINEERING

HEAT AND MOMENTUM TRANSFER FROM THE WALL OF A POROUS TUBE

H. E. Stubbs

This dissertation was submitted in partial fulfillment of the requirements for the degree of Doctor of Philosophy in the University of Michigan, 1957.

January, 1957

IP-203

ACKNOWLEDGEMENTS

This research was supported by the United States Air Force through the Air Force Office of Scientific Research, Air Research and Development Command.

The author would like also to acknowledge the contributions of the following people:

Professor Churchill and the other members of his Doctoral Committee for their advice and guidance throughout the work,

Myron Tribus, Associate Professor, University of California, Los Angeles, for his very helpful comments in the early stages of the investigation,

Bill Willis, Research Assistant, Engineering Research Institute, University of Michigan, for his excellent work in constructing the apparatus,

John Peterson, Research Assistant, Engineering Research Institute, University of Michigan, for his help in the computations with the differential analyzer.

TABLE OF CONTENTS

LIST OF FIGURES

I. INTRODUCTION

The principal purpose of this study is to give some insight into the interaction of a turbulent flow with a wall, especially for the case where the wall is porous so that fluid can pass through it. It is also hoped that the study will offer information about momentum and heat transfer rates from the walls of porous tubes.

Porous materials have recently aroused considerable interest because of the possibility of using them to contain the flow of very high temperature fluids. In such an application, a small quantity of a coolant fluid is forced through the porous wall into the region where the hot fluid is flowing. The arrangement is desirable in that the coolant is used very efficiently because it is discharged at the temperature of the hottest part of the wall, and also in that the flow field in the immediate vicinity of the wall is modified to reduce the heat transfer from the main stream to the wall. If, on the other hand, fluid is sucked from the hot flow through the wall, the flow field is modified so as to increase the heat transfer. The latter case is equally interesting from the point of view of scientific curiosity, but it does not at present offer as promising a field for applications concerning heat transfer, although it has been considered for boundary layer control in aircraft.

Most of the applications for a porous wall will be complicated by additional factors such as complex geometry, compressibility of the hot gas flowing at high velocities, variation of the properties of the fluid with temperature, or generation of heat by friction or

chemical reaction. The difficulty in analyzing any one of these additional factors is formidable in itself, and it is the plan of this study to avoid the peripheral complications as far as possible, so that attention can be focused on the effects arising essentially from flow through the porous wall.

Accordingly, a very simple case has been chosen for analysis: the flow in a smooth circular tube with uniform flow through the wall. It is assumed that the fluid passing through the wall is the same in composition as that in the main flow and that the physical properties of the fluid are uniform and constant. The flow under consideration is supposed to be far enough from the entrance of the porous tube so that effects peculiar to the entrance region can be neglected. In other words, the flow is fully developed turbulent flow.

In addition to the analysis, an experimental program was undertaken in order to give information about the applicability of the concepts of the analysis and to define its limitations. The experimental set-up was designed to avoid the complications that may attend practical situations using porous walls and to simulate so far as possible the same simple case that was considered in the analysis.

The literature pertaining to heat transfer from porous walls has been well reviewed by Broadwell and Sherman.[1] Many of the studies of the phenomena related to porous walls are concerned with laminar flow exclusively, and others deal with the flow near the leading edge of a porous plane, and therefore are not directly comparable to this study. An exception is the work of Weissberg and Berman[7] which will be discussed extensively later.

II. ANALYSIS

The purpose of this section is to show how, with suitable simplifications and approximations, the Navier-Stokes and continuity equations, which are the basic equations of fluid flow, can be simplified to give an equation descriptive of the flow in a porous tube and amenable to calculation.

At the outset, it will be assumed that the analysis is applied to a fluid whose properties are invariant. Since, under this assumption, the density plays no significant role, it will be permanently disposed of by incorporating it into the pressure, shear, or viscosity as appropriate. The "pressure" and "shear" will accordingly mean kinematic quantities with fundamental units of velocity squared, and the "viscosity" will mean kinematic viscosity.

Equations of Motion

If x, r, and φ are taken as the axial, radial, and angular coordinates, and U_i, V_i, and W_i as the corresponding velocity components, the Navier-Stokes equations are[2]

$$\frac{\partial U_i}{\partial t} + U_i \frac{\partial U_i}{\partial x} + V_i \frac{\partial U_i}{\partial r} + \frac{W_i}{r} \frac{\partial U_i}{\partial \varphi} = - \frac{\partial P_i}{\partial x} + \nu \nabla^2 U_i$$

$$\frac{\partial V_i}{\partial t} + U_i \frac{\partial V_i}{\partial x} + V_i \frac{\partial V_i}{\partial r} + \frac{W_i}{r} \frac{\partial V_i}{\partial \varphi} - \frac{W_i^2}{r} = - \frac{\partial P_i}{\partial r}$$

$$+ \nu \left\{ \nabla^2 V_i - \frac{V_i}{r^2} - \frac{2}{r^2} \frac{\partial W_i}{\partial \varphi} \right\} \qquad (1)$$

$$\frac{\partial W_i}{\partial t} + U_i \frac{\partial W_i}{\partial x} + V_i \frac{\partial W_i}{\partial r} + \frac{W_i}{r} \frac{\partial W_i}{\partial \varphi} + \frac{V_i W_i}{r} = - \frac{1}{r} \frac{\partial P_i}{\partial \varphi}$$

$$+ \nu \left\{ \nabla^2 W_i + \frac{2}{r^2} \frac{\partial V_i}{\partial \varphi} - \frac{W_i}{r^2} \right\}$$

and the continuity equation is

$$\frac{\partial U_i}{\partial x} + \frac{1}{r}\frac{\partial (rV_i)}{\partial r} + \frac{1}{r}\frac{\partial W_i}{\partial \varphi} = 0 \qquad (2)$$

(Definitions of all symbols are given in Appendix I.)

The Mean Velocity Equations

The time variation in these equations can be removed by separating the velocity components and the pressure into steady and fluctuating parts, designated by capital and lower case respectively, and then taking time averages of the several terms of the equations. This yields

$$\text{a.}\quad \frac{\partial}{\partial x}\left(U^2 + \overline{u^2}\right) + \left(\frac{\partial}{\partial r} + \frac{1}{r}\right)\left(UV + \overline{uv}\right) = -\frac{\partial P}{\partial x} + \nu\left\{\frac{\partial^2}{\partial x^2} + \left(\frac{\partial}{\partial r} + \frac{1}{r}\right)\frac{\partial}{\partial r}\right\} U$$

$$\text{b.}\quad \frac{\partial}{\partial x}\left(UV + \overline{uv}\right) + \left(\frac{\partial}{\partial r} + \frac{1}{r}\right)\left(V^2 + \overline{v^2}\right) - \frac{\overline{w^2}}{r} = -\frac{\partial P}{\partial r} + \nu\left\{\frac{\partial^2}{\partial x^2} + \left(\frac{\partial}{\partial r} + \frac{1}{r}\right)\frac{\partial}{\partial r}\right\} V \qquad (3)$$

$$\text{c.}\quad \frac{\partial}{\partial x}\overline{uw} + \left(\frac{\partial}{\partial r} + \frac{2}{r}\right)\overline{vw} = 0$$

$$\frac{\partial U}{\partial x} + \left(\frac{\partial}{\partial r} + \frac{1}{r}\right) V = 0 \qquad (4)$$

The above equations have been simplified by taking into consideration the cylindrical symmetry of the steady part of the flow.

Although the transformation of the equations eliminates the time variable functions of the velocity field, it does so at the price of increasing the number of dependent variables. The system of Equations (3) and (4) contains the average perturbations as well as the

pressure and velocity components and thus more unknowns than equations. Some further information must therefore be brought into the system in order to effect a solution. This is why later in the analysis empirical laws will be introduced.

Methods Used in Similar Problems

It will be worthwhile at this point to consider briefly the general method of proceeding in the attacks on two problems similar to the one under discussion, namely, turbulent flow with an impermeable wall and non-turbulent flow with a porous wall, to see where the peculiar difficulties of the present case arise. For turbulent flow in an impermeable tube, V and the axial derivatives of the velocity field are zero, so that the equations can be further simplified to

$$\begin{aligned} &\text{a.} \quad \left(\frac{\partial}{\partial r} + \frac{1}{r}\right)\overline{uv} = -\frac{\partial P}{\partial x} + \nu\left(\frac{\partial}{\partial r} + \frac{1}{r}\right)\frac{\partial U}{\partial r} \\ &\text{b.} \quad \left(\frac{\partial}{\partial r} + \frac{1}{r}\right)\overline{v^2} - \frac{\overline{w^2}}{r} = -\frac{\partial P}{\partial r} \\ &\text{c.} \quad \left(\frac{\partial}{\partial r} + \frac{2}{r}\right)\overline{vw} = 0 \end{aligned} \tag{5}$$

From Equation (5b) it can be seen that $\partial^2 P/\partial x \partial r = 0$. Therefore, differentiating (5a) with respect to r not only eliminates the dependent variable P, but also has the happy result of eliminating the independent variable x, and giving total differential equations

$$\begin{aligned} &\frac{d}{dr}\left(\frac{d}{dr} + \frac{1}{r}\right)\frac{\nu dU}{dr} - \overline{uv} = 0 \\ &\left(\frac{d}{dr} + \frac{2}{r}\right)\overline{vw} = 0 \end{aligned} \tag{6}$$

Obtaining equations in one independent variable is a big step towards the solution of the problem of turbulent flow in an impermeable tube,

but the difficulty of the extra dependent variable still remains, and some further supposition about the variation of the turbulence must be made to continue with the analysis.

Turning now to the problem of a tube with a porous wall but without turbulence, the perturbation terms in Equation (3) vanish. The problem has been analyzed by Yuan and Finkelstein[3] for the case when the flow through the wall is uniform. For this one special case, the variables can be separated to yield total differential equations. There are as many equations as dependent variables, and they can be solved without recourse to any empirical information.

Simplification of Equation

It can be expected then that any attempt to solve the problem of turbulent flow in a porous tube will have to accept the necessity for some empiricism in its development to cope with the added variables introduced in converting the time variation of turbulence to average values, and that in order to obtain manageable equations, some way must be found to obtain total differential equations from Equations (3) and (4).

When the turbulent perturbation terms are present as in Equations (3), it is no longer possible to separate the variables in the manner used successfully by Yuan and Finkelstein for steady flow, and a total differential equation can be obtained only as an approximation. The development of the equation is as follows. Eliminating P between Equations (3a) and (3b) gives

$$\frac{\partial}{\partial r}\left(\frac{\partial}{\partial r}+\frac{1}{r}\right)\left(UV+\overline{uv}-\nu\frac{\partial U}{\partial r}\right)+\frac{\partial}{\partial r}\left(\frac{\partial}{\partial x}\right)\left(U^2+\overline{u^2}-\nu\frac{\partial U}{\partial x}\right)=$$
$$\frac{\partial^2}{\partial x^2}\left(UV+uv-\nu\frac{\partial V}{\partial x}\right)+\frac{\partial}{\partial x}\left(\frac{\partial}{\partial r}+\frac{1}{r}\right)\left(V^2+v^2-\nu\frac{\partial V}{\partial r}\right) \qquad (7)$$
$$+\frac{\nu}{r^2}\frac{\partial V}{\partial x}-\frac{1}{r}\frac{\partial\overline{w^2}}{\partial x}$$

Those readers who are content to rely on the intuitional feeling that only the highest derivatives with respect to r are important and that as a consequence all but the first term of Equation (7) can be neglected, can pass on to Equation (16) where they will find that their intuition is correct. The more skeptical are asked to suppose that the variables can be separated approximately and that the velocity can therefore be normalized with a friction velocity $\sqrt{\tau}$ in the same way as for the case of the impermeable wall. The equations describing the normalization are

$$U = U^* \sqrt{\tau} \qquad (8)$$

$$y = a - r = y^* \nu/\sqrt{\tau} \qquad (9)$$

The supposition that u^* is a function of y^* alone can now be shown to be compatible with Equation (7) except for very small terms. To facilitate the analysis, it is assumed that $\sqrt{\tau}/U_b$ is a constant so that

$$\frac{d\sqrt{\tau}}{dx} = \frac{\sqrt{\tau}}{U_b}\frac{dU_b}{dx} = \frac{4V_w}{DU_b^*} \qquad (10)$$

and

$$\frac{d^2\sqrt{\tau}}{dx^2} = 0 \qquad (11)$$

This is not strictly so, for $\sqrt{\tau}/U_b$, which is square root of the friction factor, varies somewhat with the Reynolds modulus and thus with x, but the variation is small and can be reasonably neglected in an order analysis. Some of the terms of Equation (7) can be expressed thus:

$$\frac{d^2}{dr^2}\ \frac{\nu dU}{dr} = \frac{\tau}{D^2}\ \frac{Re}{U_b^*}^2 \left\{\frac{d^3U^*}{dy^{*3}}\right\} \tag{12}$$

$$\frac{d^2}{dr^2}\ \overline{uv} = \frac{\tau}{D^2}\ \frac{Re}{U_b^*}^2 \left\{\overline{u^*v^*}\right\} \tag{13}$$

$$V\ \frac{d^2U}{dr^2} = V^*\ \frac{\tau}{D^2}\ \frac{Re}{U_b^*}^2 \left\{\frac{d^2U^*}{dy^{*2}}\right\} \tag{14}$$

$$\frac{d^2}{drdx}\ U^2 = \frac{\tau}{D^2}\ \frac{Re}{U_b^*}\ \frac{4V_w}{U_b}\ \left\{6U^*\ \frac{dU^*}{dy^*} + 2y^*U^*\ \frac{d^2U^*}{dy^{*2}} + 2y^*\ \frac{dU^*}{dy^*}^2\right\} \tag{15}$$

The above terms permit some general evaluations to be made. All the evaluations are based on the velocity field which is known experimentally for V = 0. When V is not zero the values will change, but if the Reynolds modulus remains the same and the velocity through the wall is small compared to that in the tube, it is reasonable to expect that the values of U^*, U_b^*, and $\sqrt{\tau}$ will not change by orders of magnitude. A final check of this assumption can be made when the analysis is completed giving the velocity profile as a function of V.

Comparison of Terms

In comparing the terms, it is convenient to consider separately the functions of y^* which are enclosed in $\{\ \}$ and the constants which precede the function. Taking the functions first, U^* is zero at $y^* = 0$. It then increases continuously with y^* but rather slowly

at larger values. It is about 25 for y* of 1500. dU^*/dy^* is a maximum of 1 when y* is 0. d^2U^*/dy^{*2} has a maximum of about .1 at y* = 10. The third derivative of experimental data is rather uncertain, but it appears that d^3U^*/dy^{*3} has a maximum of about .02 at y* = 5. $\overline{u^*v^*}$ is equal to 1 - dU^*/dy^*. Accordingly, the functions of y* and U* which appear in the different terms differ from each other by factors less than 100. An exception to this is the third derivative which becomes quite small for larger values of y*.

Turning to the constants, Re/U_b^* can best be conceived of as D*, the non-dimensional diameter. At reasonable values of Reynolds modulus, it is large; for example for Re = 50,000, D* is about 2600. The factor V_w/U_b is a measure of the flow through the walls, which for the gases under consideration will be such that the flow in the tube changes slowly--about 1 percent per diameter or less. The corresponding values of V_w/U_b are .0025 or less. The constant $V_w^* = U_b^*(V_w/U_b)$ and so will be about .05. It can be seen that as far as the constants are concerned, the terms $(d^2/dr^2)(dU/dr)$ and $(d^2/dr^2)\overline{uv}$ are the same magnitude. This is to be expected, since these two terms are the ones that are significant when V = 0. They can serve as a standard for comparison of the other terms of the equation. Next it can be seen that any term with an x-derivative in it has a factor of $(U_b^*/Re)(4V_w/U_b)$ as compared to the standard terms. By the estimate above this factor is .000004 and, since the functions of y* differ by at most a factor of 100, any term containing an x-derivative can be neglected. The terms without an x-derivative in the equation thus give

$$\frac{d}{dr}\left(\frac{d}{dr} + \frac{1}{r}\right)\left(UV + \overline{uv} - \frac{\nu dU}{dr}\right) = 0 \quad . \qquad (16)$$

Integrating Equation (16) and taking account of the boundary conditions:

$$U = uv = 0 \text{ at } r = a \tag{17}$$

$$V = \frac{dU}{dr} = 0 \text{ at } r = 0 \tag{18}$$

gives the equation

$$UV + \overline{uv} - \frac{\nu dU}{dr} = \frac{r}{a}\sqrt{\tau} \tag{19}$$

or in non-dimensional form

$$U^*V^* + \overline{u^*v^*} + \frac{dU^*}{dy^*} = \frac{r}{a} \tag{20}$$

The last equation can be further simplified by supposing V to be a constant and r/a to be 1. The justification for doing this is not so good as that for neglecting the terms having an x-derivative, and the supposition is certainly wrong near the center of the tube, but it is justifiable near the wall. The variation in V can be estimated from Equation (4) which is convenient to transform thus:

$$\frac{d}{dr}(rV) = -\frac{d}{dx}\left(r\frac{U^*}{U^*_b}U_b\right) \doteq r\frac{U^*}{U^*_b}\frac{dU_b}{dx} = \frac{2V_w}{aU^*_b}rU^* \quad .$$

The results of integrating the equation for the limiting case as V approaches 0 and with the Reynolds modulus 50,000, is shown below.

y^*	0	10	20	60	200
V/V_{wall}	1.00	1.00	1.00	.99	.91

There is little variation in U* near the center of the tube anyway, and it is not important to calculate changes in velocity accurately in this region if only the value of U is required. Furthermore, the suppositions about the turbulence which must be introduced later in the analysis are rather crude and thus preclude a very accurate solution in any event. The argument may be summed up by saying that taking V

as a constant and r/a as 1 gives a simpler equation that is approximately right where it needs to be right. The final form of the equation of motion which will form the basis for further computations is then

$$U^*V^* + \overline{u^*v^*} + \frac{dU^*}{dy^*} = 1 \quad . \tag{21}$$

Interpretation of Simplified Equation

Equation (20) (or its simpler form, 21) indicates that the primary effect of the radial component of velocity is to alter the non-dimensional shear given by the terms $(\overline{u^*v^*} + \frac{dU^*}{dy^*})$. With no flow through the wall the shear is uniform (or decreasing very gently according to the more complete Equation 20). In contrast, with flow through the wall, the shear is augmented by the quantity $-V^*U^*$. This is illustrated in Figure 1, where the shear and velocity are plotted against the same y^* coordinate.

The Turbulent Term in the Equation

In order to advance the analysis further, it is necessary to express the turbulence term, $\overline{u^*v^*}$, as some function of the variables U^* and y^*. This expression will represent the additional information that must be brought into the system of differential equations because of the averaging process which was used to eliminate the time variation. Our understanding of turbulence is still quite meager, and the best that can be hoped for in an analysis of flow in a porous tube is a generalization based on measurements made in flows in impermeable tubes.

The expressions for $\overline{uv}$ that will be considered here are usually referred to as mixing length theory. The argument for the expressions is essentially a rationale based on dimensional analysis. The original

proposal of the mixing length theory came from Prandtl, and he suggested that near the wall the velocity field would be characterized principally by the velocity gradient and the distance to the wall. Accordingly, he proposed an expression $\overline{uv} = -(Ky\, dU/dy)^2$ in which K was to be determined experimentally. Von Karman later proposed that at some distance from the wall the flow would so to speak be "unaware" of its absolute velocity or the distance to the wall, and that the flow field would be characterized by the first and second derivatives of the velocity. The expression corresponding to this view is

$$\overline{uv} = -\left\{\frac{K(dU/dy)^2}{d^2U/dy}\right\}^2$$

where again K was to be determined from experiment. It can be seen that each of the expressions is the only dimensionally correct expression formed from the quantities that are considered most important for characterizing the turbulent flow. There are, of course, other properties (such as higher derivatives), and the argument for the expressions is not rigorous, but they are eminently sensible if somewhat crude.

In the development of a law for the velocity variation in an impermeable tube from either expression, the effect of viscosity was neglected in the region away from the wall, and the solution thus obtained was patched onto a viscous solution for the region immediately adjacent to the wall. With this treatment, the two expressions for turbulence yielded the same law for the variation of the velocity, and there was little incentive to discriminate between them. The identity of results from the two laws is, however, fortuitous, and they do not give identical results in an analysis of the flow field

near a porous wall (in fact, not even for an impermeable wall if viscous effects are included). It is therefore important to compare the two expressions against experiment in the region where both turbulence and viscosity are significant to see which better represents the flow field. The opportunity to do this is far better today than it was when the expressions for turbulence were proposed, because the critical comparisons involve derivatives of the velocity. The earlier investigators of turbulent flow measured the mean velocities, and although their work was careful, it is not up to yielding a second derivative. More recently, the turbulent component $\overline{uv}$ has been measured, and this is equivalent to obtaining a direct measurement of the first derivative of the velocity curve. In particular, Laufer's experiments are most helpful.[4] It is clear at the outset that the von Karman expression cannot be correct at the wall because it does not give a value of zero for the turbulence at the wall. A comparison of the two expressions for turbulence against the measurements of Laufer is shown in Figure 2 for the region in which the effect of viscosity is enough to distinguish the two forms. The Prandtl and von Karman curves were obtained by putting values of y^*, U^*, and the derivatives of U^* from Laufer's curves[4] into the Prandtl and von Karman expressions. The von Karman curve is somewhat uncertain because it depends on the second derivative of the velocity which is hard to obtain accurately. It can be seen, however, that the von Karman expression is definitely better than that of Prandtl, and that the von Karman expression is in pretty good agreement with experiments for values of y^* greater than 20.

The argument supporting the von Karman expression holds with equal force when there is flow through the wall of the tube, so that

there is a reasonable presumption that it will give a good estimate of the turbulent term, $\overline{uv}$, in the region y* greater than 20 for a porous tube. Accordingly, the von Karman expression will be used for y* greater than 20, with the constant K taken the same as in an impermeable tube, about .4. Incorporating the von Karman expression into Equation (21) gives

$$\frac{d^2U^*}{dy^{*2}} = - \frac{K\left(\frac{dU^*}{dy^*}\right)^2}{\sqrt{1 - \frac{dU^*}{dy^*} - V^*U^*}} \qquad (22)$$

For y* less than 20, neither the Prandtl nor the von Karman expression is correct, and something else must be used.

In the region y* less than 20, the turbulent structure is complicated by the interaction of the turbulent motion and the wall. It is fairly clear that the distance to the wall as well as the derivatives of the velocity field is important in characterizing the behavior of the flow. With this added complexity the dimensions of velocity squared which are required for the turbulent term in the equation of motion can be formed in a variety of ways, and the dimensional argument which was helpful in the previous instance does not offer any guide.

Besides the dimensional considerations, about all that is known of the turbulence near the wall is that it must become zero at the wall and that it must reduce to the known pattern for an impermeable wall when V becomes zero. The simplest rule that satisfies these conditions is that the total shear at any point near the wall be divided in the same ratio between the viscous and the turbulent mechanisms as for an impermeable wall. The distance from the wall in this

context means as measured by y*. An equivalent statement for variation of the turbulence is that ratio of the eddy viscosity to the viscosity is a function of y* only and independent of V in the region y* less than 20. The rule receives some support from the consideration that the most important thing that happens in this region of the tube is the interaction of the wall with the turbulence present in the main part of the flow. The turbulent motion thus is suppressed as it comes nearer the wall. It seems reasonable that this interaction should not be drastically altered by a small flow through the wall. It must, however, be conceded that the argument is less convincing than that for the von Karman expression in a region farther from the wall. The symbolic representation of the turbulence in the region y* less than 20 is thus

$$f(y^*) = \frac{\overline{u^*v^*}}{\frac{dU^*}{dy^*}} \tag{23}$$

where $f(y^*)$ is determined from the measurements made in a tube with an impermeable wall.

Method of Solution of the Equation

Once the turbulence term is expressed as a function of U* and y*, the solution of Equation (21) is pretty much mechanical. For the range y* less than 20, substitution of Equation (23) into (21) gives

$$\frac{dU^*}{dy^*} = \frac{1 - V^*U^*}{f(y^*) + 1} \tag{24}$$

The values of $f(y^*)$ were calculated from Laufer's paper, and the solution was obtained by increments starting at y* = 0, where U* = 0 and $dU^*/dy^* = 1$.

For the range y* greater than 20, the computation of Equation (22) was made on an electronic differential analyzer. Details of the circuitry are given in an appendix.

Determination of the Constant K

As preliminary to the calculation with flow through the wall, the velocity field was calculated for an impermeable wall. This offered an opportunity to check the method of solution against the well-known experimental velocity profile and also to determine the best value for the constant K about which there has been some disagreement in the past. The velocity profile computed with three values of K and some representative experimental points are shown on Figure 3. It appears that the plot of U* vs y* does not depend critically on K. The value .38 appears to be about the best for representing the experiments. It is used in the succeeding computations.

The Assumption that V is Constant

Another question which was examined was whether a serious distortion of the profile was made by the assumption that V was a constant. To obtain some estimate of the effect of variation of V during the course of the computation, U* was computed from Equation (22) from y* = 0 to y* = 200. Then the computation was halted and the differential equation changed by setting V = 0, after which the computation of U* was continued out to y* = 1500. The results are compared with that obtained when V was considered constant throughout in Figure 4. In interpreting Figure 4, it should be remembered that the variation introduced in V in the one procedure is considerably greater than that which really occurs in a tube. The true velocity profile will lie between the two curves that appear in Figure 4 and closer to the one with

constant V. Keeping this in mind, it can be seen that the assumption of constant V does not produce an important distortion.

The Velocity Profiles

The plots of U* against y* are shown in Figure 5 with a y* scale of 150 and in Figure 6 with a y* scale of 1500. (The points that appear on these figures will be discussed later, in the chapter on experimental work.) In thinking about the curves, it should be remembered that the effect of using the variables U* and y* is to make all curves have a slope 1 at the wall.

The most important features of the velocity profiles are that the curves with negative V (blowing into the tube) show a larger region near the wall in which the velocity rises steeply. Furthermore, the slope of a curve with lower V is greater throughout than that of a curve with a higher V. The result is that curves with a negative V rise considerably higher, and those with a positive V are very flat away from the wall. Another characteristic of the curves that is important although not so obvious to a casual glance is that the second derivative of the curves with a negative V is greater than zero at the wall and passes through zero to form a point of inflection at a little distance from the wall. The negative second derivative (at about y* = 20) is evident; the positive second derivative at the wall can be verified by differentiating Equation (21), remembering that the turbulent term is at least a second order zero at the wall.[4]

Application to Heat Transfer

If the Reynolds analogy between heat transfer and fluid friction is accepted, the analysis can be interpreted directly in terms of thermal quantities. More sophisticated treatments of the heat transfer

phenomena could be attempted, but in view of the simplifications that have been made elsewhere in the analysis, especially concerning the turbulence, it is doubtful if they would produce significantly better results. The analogy has well-known deficiencies, but it is still quite reasonable for fluids with Prandtl modulus near 1.[5]

The quantity corresponding to U* is

$$U^* = t^* = C(t - t_w) \frac{\tau}{q} \tag{25}$$

where t is the temperature, and the density has been incorporated into the heat capacity C which is accordingly the heat capacity per unit volume at constant pressure. The heat flux density q defined as

$$q = k \left(\frac{dt}{dy}\right)_{wall} \tag{26}$$

represents the thermal energy that is transferred from the wall by conduction. In an impermeable tube, conduction is the only way to transfer heat from the wall, but with a porous wall another mechanism for the transfer of thermal energy is available, which might be called the convective component since it is associated with the gross movement of the fluid and is proportional to the fluid's heat capacity. The convective component is, however, dependent on the reference state chosen for the fluid and an alternative view is that q is the heat transferred from the wall when the reference state for the fluid is taken as having the temperature of the fluid at the wall. The analogous problem for friction was unobtrusively disposed of by assuming the wall of the tube to be at rest.

Bulk Properties

While the plot of U* = t* against y* in Figures 5 and 6 includes implicitly all the information about the steady state flow, it is frequently convenient to have explicit information about the bulk properties of the flow. The bulk velocity (defined as the ratio of the volume flow through the tube to the cross-sectional area) can be obtained from the velocity plot

$$U_b = \frac{2}{a^2} \int_0^a U\, r\, dr \tag{27}$$

or in terms of starred variables

$$U_b^* = \frac{2}{a^*} \int_0^{a^*} U^* dy^* - \frac{2}{a^{*2}} \int_0^{a^*} U^* y^* dy^* \tag{28}$$

U_b^* is plotted against a*, the non-dimensional radius, for several values of V* in Figure 7. Lines of constant Reynolds modulus, which is related to the *-variables by

$$Re = \frac{2aU_b}{\nu} = 2a^* U_b^* \tag{29}$$

are also plotted in the same figure.

Another bulk property that is particularly important because it involves the variables of the flow which are most accessible to measurement and most useful in design is the friction factor.

$$f = \frac{2\tau}{U_b^2} = \frac{2}{U_b^{*2}} \tag{30}$$

This is plotted against V/U_b with Reynolds modulus as a parameter in Figure 8.

The bulk thermal properties of the flow are based on the mean temperature of the stream t_m. This is defined so that enthalpy calculations for the stream come out right

$$t_m = \frac{2}{a^2 U_b} \int_0^a t\, U\, r\, dr \qquad (31)$$

or in non-dimensional variables, and taking note of $t^* = U^*$

$$t_m^* = \frac{2}{U_b^*} \left\{ \frac{1}{a^*} \int_0^{a^*} U^{*2} dy^* - \frac{1}{a^{*2}} \int_0^{a^*} U^{*2} y^* dy^* \right\} \qquad (32)$$

It should be noted that t_m^* is not analogous to U_b^*. Using Equation (32), t_m^* can be calculated graphically from the plots of U^*. (See Figure 9).

The Nusselt modulus is readily obtained from t_m

$$\frac{2a}{k} \quad \frac{q}{t_m - t_w} = \frac{2a^*}{t_m^*} \quad \frac{C\nu}{k} \qquad (33)$$

and is plotted in Figure 10 for $C\nu/k$ equal to 1.

Recapitulation of Analysis

The most important conclusions of the analysis are that the equations governing flow in a porous tube can be reduced by reasonable approximations to simpler equations that are amenable to solution by difference methods or with a differential analyzer. The most critical step in the process is the representation of the turbulent term in Equation (21) by an empirical relationship taken from measurements on flow in an impermeable tube in the region close to the wall, and with an expression based on dimensional analysis in the region farther from the wall.

The principal effect of the flow through the wall is to make the shear in the fluid vary rapidly with the distance from the wall, whereas without flow through the wall, the shear is approximately uniform near the wall.

The solution of the simplified equations yields velocity profiles for the flow and values of friction factor for various values of the Reynolds modulus and the flow rate through the wall. If the analogy between momentum and heat flux is applicable, the solution can also be interpreted to give temperature profiles and the Nusselt modulus. It can be expected from the nature of the assumptions made in simplifying the equations that the solutions will be better approximations for the higher values of Reynolds modulus and for values of the flow through the walls closer to zero. A further condition applicable only to the thermal quantities is that the Prandtl modulus be close to 1.

III. EXPERIMENTAL WORK

Choice of Experimental Work

Since the first object of the experimental work contemplated here is to outline the limitations of the theoretical work of the preceeding section, it might seem at first thought that measurements of velocities and momentum fluxes would be the best way to check the analysis, inasmuch as these are the quantities with which the analysis is most directly concerned. The measurement of the momentum flux at a wall is, however, far more difficult than the measurement of heat flux, and this consideration proved conclusive in the decision to conduct a series of experiments on heat transfer from a porous tube.

It was further decided that it would be better to check the theory in terms of its prediction of the bulk characteristics of the flow which are more easily measured and give nearly as much information about the flow field as would measurements of profiles.

The Apparatus

The essential features of the experimental apparatus are shown in Figure II.* After passing through an entrance section some 80 diameters long, in which it acquired the profile of fully developed turbulence, the primary stream of air passed through the porous section, which is 18 diameters long, and out through the exit section. All of the above tubing was 1 inch inner diameter. A second stream of air supplied a plenum chamber around the porous tubing. Air flowed from the plenum chamber uniformly through the porous wall of the tube. Electrical connections were made to either end of the porous tube so that the tube could

---

* The description given here is simplified considerably in order to give conceptual clarity. A full description is given in an appendix.

be heated uniformly over its surface by the passage of electric current. The secondary air stream, which supplied the plenum chamber, could also be heated. Thermocouples measured the temperatures in the two inlet streams, the outlet stream, and in the wall of the porous tube near its downstream end. The flow in the two inlet streams and the power dissipated in the porous tube were also measured. The data obtained from the experiment were thus the temperature and flow of each stream, the heat dissipated in the wall of the tube, and the temperature of one point of the wall of the tube.

Equivalence of Experiment and Analysis

In order to make the experiments easily comparable with the theory, it was important to make the experimental situation correspond as closely as possible to the idealized system which was analyzed. As mentioned above, the measurement of the wall temperature was well down stream from any entrance irregularities to conform to the neglect of entrance conditions in the theory. Air was used as the fluid because it was convenient and has a Prandtl modulus close to 1. The temperature differences in the tube were maintained in a range around 5°C because within this range the properties of the fluid are approximately invariant as assumed in the analysis. At the same time, the temperature differences arising from viscous heating, which were neglected in the analysis, were negligibly smaller than those arising from heat flux from the wall.

One difficulty in designing experiments which simulate the analysis is less evident. The "wall temperature" designated t_w which appears in the analysis is, as is clear from the context, the limiting temperature of the fluid in the tube as the distance to the wall approaches zero. This is not necessarily the same as the temperature of the solid material of the wall or the temperature which a thermocouple

imbedded in the wall will indicate. Although a paper by Weinbaum and Wheeler[6] indicates that the wall and the gas are very close to the same temperature, preliminary experiments with the porous tube used in this study showed that the air passing through the wall could issue at a temperature appreciably different than that of the wall. To insure therefore that the air did issue from the wall at the temperature of the wall and thermocouples, the temperature of the air in the plenum chamber was adjusted in all cases to be the same as that of the wall.

Finally there is the question of how well the surface of the tube used in the experiments corresponds to the analysis. In the analytical model, fluid issues uniformly from a smooth, well defined boundary. In the experiments, the fluid squirts out of many irregular little hole in the wall, and on a microscopic scale, the flow through the wall is certainly not uniform, nor is the surface of the wall clearly defined. The discrepancy cannot in principle be reconciled, for fluid must have holes to pass through a wall, and an analysis that looks at thousands of individual holes is not feasible. One can only say that if the structure of the wall is fine enough, the flow from it will probably correspond to that of the model. Although the structure of the tube wall used in these experiments was far finer than the tube diameter, there is still some doubt whether it was fine enough, for, turbulence being essentially a manifestation of instability in the flow, there is the possiblity that small causes can produce large effects. The question whether the phenomena found in the experiments are sensitive to the structure of the wall must therefore be left open.

Heat Leaks

Another important consideration in the design of the experimental set-up was the control of heat leaks. Generating the heat in the

tube itself by an electric current is a very effective way of insuring that all the metered energy goes into the gas flow, rather than being lost in any ducts. The system described has a further advantage that any heat conducted outwards into the gas of the plenum chamber is swept back to the tube by the motion of the gas, making the plenum chamber an excellent insulator.

Calculations From Experiments

With the aid of enthalpy balances, the Nusselt modulus, defined by:

$$Nu = \frac{2a}{k} \frac{q}{t_m - t_w}$$

can be calculated for the point of the tube where the temperature was measured. An enthalpy balance over the portion of the porous tube upstream from the point where the wall temperature is measured gives the total enthalpy flow of the gas stream at this point. Similarly, a mass balance gives the total mass flow. From these two quantities the bulk (or mixed mean) temperature at the point of the thermocouple can be calculated, and from that the denominator of the Nusselt modulus. Another enthalpy balance around the increment of wall whose temperature was measured gives the numerator of the Nusselt modulus:

$$q = \frac{\text{electric power}}{\text{area of wall}} + CV\,(t_p - t_w) \qquad (34)$$

where t_p designates the temperature of the air in the plenum chamber. Details of the calculation appear in an appendix.

Results of Experiments

The results of the experiments are shown in Figure 10 where they can be compared with the theoretical results. For small values of flow through the wall the experimental points fall close to the

analytical curves, and the curves appear to give a correct representation of the slope of the data in the vicinity of zero flow. At higher flows, however, the data deviate appreciably from the analysis, and it appears that the Nusselt modulus changes very slowly with further increase of the flow through the wall. The divergence of experiment and analysis becomes important when the parameter V^* exceeds about .02 in all cases. The data for all values of the Reynolds modulus can be brought together fairly well by plotting $Nu/(Re)^{.8}$ against V/U_b as shown in Figure 12. A further discussion will be undertaken after a review of some experimental work from another source.

Experiments with Suction

Weissberg and Berman have measured velocity profiles and longitudinal pressure variation in the turbulent flow in a tube from which air was being sucked[7], which can also be used for comparison with the analysis presented here. They did not, however, measure the shearing stress on the wall of the tube, and in order to form non-dimensional quantities corresponding to the quantities within this paper, they used values for the shear at the wall obtained from an empirical formula. The formula implies that the shear is independent of the flow through the wall, and thus is incompatible with the central question of this study, which is how the shear varies with the flow through the wall. Weissberg and Berman themselves state that their own measurements of the pressure drop indicate that the shear is dependent on the flow through the wall. The use of this spurious shear confuses the picture of the velocity profiles, and the Weissberg and Berman data must be reinterpreted before they can be compared with the analytical results of the preceeding section.

Reinterpretation of Weissberg and Berman Data

In outlining the method for revising the interpretation of the Weissberg and Berman data, it is necessary to distinguish between the shear velocity at the wall as computed by the formula, designated by u_s, and that obtained from the analysis of this study, which as before is designated $\sqrt{\tau}$. In Figure 15 of the Weissberg and Berman paper the quantity U/u_s is plotted against yu_s/ν. A plot of $U/\sqrt{\tau}$ against $y\sqrt{\tau}/\nu$ is what is needed. The conversion to the desired plot is summarized in the following table.

1 Run	2 Re	3 u_s/U_b	4 V/u_s	5 $1000V/U_b$	6 $U_b/\sqrt{\tau}$	7 $u_s/\sqrt{\tau}$	8 $V/\sqrt{\tau}$
6-16-1	27400	.0566	.0131	.74	16.6	.940	.0123
6-14	27400	.0566	.0352	1.99	14.9	.843	.0297
6-20	27400	.0566	.0885	5.00	12.3	.694	.0614
6-13	39800	.0528	.0496	2.62	14.6	.769	.0382

Columns 2 and 4 are taken directly from the Weissberg and Berman paper. Column 3 is calculated from Weissberg and Berman Equation 16:

$$(u_s/U_b)^2 = .001876 + 36.51/Re \qquad (35)$$

Column 5, which is obtained from Columns 3 and 4, and Column 2 can be used in conjunction with the analysis of this paper represented in Figure 8 to calculate $U_b/\sqrt{\tau}$ in Column 6. Column 7, which is something of a correction factor, can be calculated and used to obtain the non-dimensional velocity and distance variables which are designated by a *. The results are plotted on Figures 5 and 6 where they can be compared with the velocity curves of the analysis.

Treatment of the data in the foregoing manner does not produce as critical a comparison with the analysis as might be desired, because it is necessary to normalize the measurements with a value of shear taken from the analysis. It would be better if an experimental measurement of the shear were available so that the *-variables could be formed entirely independently of the theory. However, with what is available, the above treatment is the best that can be achieved.

It can be seen that the analytical curves correspond quite well with the data in the range $20 < y^* < 1500$. For smaller values y^*, the Weissberg and Berman data fall below the analytical curves of the velocity profile, but the Weissberg and Berman data for an impermeable wall are also lower than that of most other experimenters, so that the result in this range is not conclusive.

Comparison of Experiments and Analysis

The comparison of the experimental and analytical results shows that the analysis is substantially correct in predicting the behavior of the flow field in a porous tube when the flow through the wall is small, and that its range of accuracy extends to a value of about .02 in the parameter V^* for blowing into the tube. With sucking from the tube, it appears that the accuracy of the analysis extends to larger values of the parameter V^*, but the experiments are less critical for the case of suction.

For blowing beyond the range of applicability of the analysis, the heat transfer properties of the flow vary more slowly than predicted. On grounds that are intuitive but still very strong, it can be expected that the velocity profile has no exotic kinks in it but rather is a very smooth curve even at high rates of flow through the wall. In view of this, the slow change in the Nusselt modulus indicates that the velocity

profile is changing only very slightly as the flow through the wall increases.

The general pattern of the behavior of the flow is illuminated by reference to Equation 21 which may be rewritten:

$$(dU^*/dy^*) + \overline{u^*v^*} = 1 - U^*V^* \qquad (36)$$

With increased blowing into the tube, (negative V*), the right side of the equation increases at any particular y*. For small values of velocity through the wall, the flow field accomodates itself by changing the velocity profile while the turbulent structure for an impermeable wall as assumed by the analysis continues much the same. At higher flows through the wall, however, the velocity profile changes little, and the increase of shear represented by the right side of the equation is accomodated by an increase in the turbulent action. With suction, the turbulent structure assumed by the analysis continues to larger flow rates.

IV. CONCLUSIONS

The analysis of the equations of motion shows that the principal effect of a flow through the wall of a porous tube is to change the pattern of momentum and heat flux in the neighborhood of the wall, and that other effects can reasonably be neglected. The shear stress and heat flux vary rapidly with distance from the wall when there is flow through the wall, whereas they are approximately uniform near the wall of an impermeable tube.

For small flows through the wall of the tube the velocity profile, friction factor, and Nusselt modulus for the tube can be calculated assuming that the structure of the turbulence in the tube is the same as for an impermeable tube. The limits of applicability of the calculation are approximately at $V^* = .02$ for blowing into the tube and somewhat higher for sucking from the tube. For greater flows in through the wall the turbulent structure of the flow is altered substantially.

Blowing into a porous tube reduces the heat transfer coefficient in the tube as shown in Figure 10. A reduction of about 13 percent is accomplished by blowing with a velocity about .001 of the bulk velocity in the main stream. Blowing with greater velocities has progressively less effect.

APPENDIX I

DEFINITION OF SYMBOLS

a	Radius of tube
C	Volumetric heat capacity (units: energy/volume-temperature)
D	Diameter of tube
f	Friction factor = $\tau/2U_b^2$
	Also used to indicate "function of"
K	Constant in expression for turbulence
k	Thermal conductivity of fluid
P	Average kinematic pressure (units: velocity squared)
P_i	Instantaneous kinematic pressure (units: velocity squared)
q	Heat flux density at wall (units: energy/area-time)
r	Radial coordinate in tube
t	Temperature of fluid (also time)
t_m	Mean temperature of stream, see Equation (31)
t_w	Temperature of fluid at wall
U	Average of axial velocity
u	Turbulent perturbation of axial velocity
U_i	Instantaneous axial velocity,
U_b	Bulk velocity, see Equation (27)
u_s	See Equation (35)
V	Average of radial velocity
v	Turbulent perturbation of radial velocity
V_i	Instantaneous radial velocity
V_w	Velocity at the wall

x Axial coordinate

y a - r

τ Kinematic shear at wall (units: velocity squared)

φ Angular coordinate

∇^2 Operator: $\frac{\partial^2}{\partial x^2} + \frac{1}{r}\left(\frac{\partial}{\partial r}\right)\left(r\,\frac{\partial}{\partial r}\right) + \frac{1}{r^2}\,\frac{\partial^2}{\partial \varphi^2}$

$*$ Indicates variable has been made non-dimensional according to this scheme:

quantity	divided by
length	$\nu/\sqrt{\tau}$
velocity	$\sqrt{\tau}$
temperature (temperature is taken with reference to wall)	$q/C\sqrt{\tau}$

$\overline{}$ Indicates time mean of quantity underneath

APPENDIX II

ANALOG CIRCUITRY

The circuit used in the differential analyzer to compute the velocity profile is shown in Figure 13. The original differential equation (21) which is

$$\frac{d^2U^*}{d^*y^2} = \frac{-k\left(\frac{dU^*}{dy^*}\right)^2}{\sqrt{1 - \frac{dU^*}{dy^*} - V^*U^*}}$$

is converted to an equivalent one for the machine by the following transformations of variables:

$$U^* = 40\ U$$

$$\frac{dU^*}{dy^*} = \frac{Z}{2}$$

$$dy^* = 100\ Y = 100\ b\ dt$$

Unstarred variables in this case indicate machine variables. The resulting differential equations are

$$\frac{1}{10b}\frac{dU}{dt} = -\frac{Z}{8}$$

$$\frac{1}{10b}\frac{dZ}{dt} = -2\frac{k}{.4}\frac{Z^2}{\sqrt{1 - \frac{Z}{2} - \frac{V}{.05}U}}$$

The only thing unusual in the circuit is the ganged potentiometer which controls the voltage input to every integrator. In effect, it controls the rate of increase of the independent variable. At low values of Y, Z changes very quickly, whereas for large values of Y nothing changes very rapidly. By setting the ganged potentiometer low at the beginning of a calculation, the servos were not required to change faster than

their capacity. Then increasing the setting of the potentiometer as the calculation proceeded made it unnecessary to wait an excessive time for completion of the run.

The circuit is shown as it was used for a range of 1500 in y^*. For a 150 range the inputs to the V and Z integrators were increased by a factor of 10.

APPENDIX III

DETAILS OF EXPERIMENTAL WORK

This section is written to describe details of the experimentation which are probably of little interest to most readers, but which may be helpful for those who wish to make similar experiments or who may wish to evaluate for themselves the reliability of the results of this investigation.

Measurement of Bulk Properties

Experimental work which might be undertaken to define the limitations of the analysis can be considered in three general catagories— bulk measurements of momentum or heat transfer, measurements of the velocity or temperature profiles and measurement of average values of turbulent perturbations such as $\overline{u^2}$ and $\overline{uv}$ or corresponding thermal quantities. There is a substantial increase in the equipement required for the catagories in the order they are listed.

Bulk measurements, which were chosen for the experimental program, give essentially the slope of the profile at the wall and the integral under the profile curve. Since the profile is certainly flat near the center of the tube and has a smooth curvature, it is pretty well defined by the information from the bulk measurements. There will, of course, be some uncertainty whether the profile has a small bulge in one place compensated by a flat somewhere else, but it is reasonable to say that the uncertainty in the location of the profile will be something like $\pm$ 10%.

Measurement of velocity of temperature profiles would provide greater accuracy than bulk measurements, but judging from the scatter of

data of investigators who have measured profiles in impermeable tubes and from the variance in the reports of the several investigators, there would still be an uncertainty of perhaps $\pm$ 5% in locating the profile in the critical region near the wall. It must be remembered that profile measurements would have to be made on a porous tube that is not nearly as perfect geometrically as those used for investigations of flow in an impermeable tube. Furthermore, profile measurements are not adequate for determining the gradient of the curve. The gradient at the wall is the key parameter in the analysis and an accurate value for it is necessary for an acute comparison of experiment and analysis. At the same time it is most difficult to obtain the gradient just at the wall, not only because it is always difficult to obtain differentiable data (and especially at the end of a curve) but also because as the measuring instrument approaches the wall its operation is affected by the wall. It appears therefore that direct profile measurements would have to be supplemented by measurements of heat or momentum flux from the wall and that they would give little information beyond that obtainable from bulk measurements.

Measurement of turbulent perturbations would give direct information about the structure of the turbulence which would undoubtedly be valuable. It requires, however, very considerably more equipment than the other experiments, and in view of the relative ignorance of even the grosser phenomena of flow adjacent to porous surfaces, it seemed better to exploit the easier bulk measurements for the present.

Having decided on bulk measurements, it was further decided to measure thermal quantities because the heat flux from a wall is much easier to obtain than the momentum flux.

The Porous Tube

One of the greatest difficulties in this whole study was the production of a tube with sufficiently uniform porosity so that measurements made on it would be meaningful. Manufacturers' specifications notwithstanding, uniformly porous metals do not seem to be available. The tube used in these experiments was made by packing Plexiglass powder in a stainless steel tube obtained from Poroloy Equipment, Incorporated. The tube was 1 inch inner diameter, 18 inches long, and had a wall thickness about .1 inch. Although details of the manufacturing process have not been revealed by the manufacturer, the tube was evidently made by weaving wires on a form and then sintering. The structure was somewhat coarser than porous sheet made from powder. On arrival, the porosity of the tube varied by about 50% from one place to another. In a very tedious operation, the porosity of the tube was leveled out by packing tiny Plexiglass beads into the wall of the tube in the areas of high porosity. Finally the variation in porosity was reduced to $\pm$ 5% in the downstream half of the tube and $\pm$ 10% in the upstream half. More precisely, for any fixed pressure drop across the wall, the flow through any part of the wall defined by a quarter inch circles was within 5% of the mean flow in the downstream half of the tube and within 10% of the mean in the upstream half. After the beads were in place, the tube was washed lightly with amyl acetate in the hope that this would cement the beads in place. Whether because of the wash or some other reason, the emplacement of the beads did prove stable, for the flow characteristics of the wall showed no appreciable change after the wall had been subjected to rapid pressure variations and reverse flows.

The method described above for tailoring the porosity of the tube was preceeded by a number of less successful attempts. These efforts

did not yield any coherent picture of the flow through porous walls or how to control it, but one of the failures was interesting enough to deserve some mention. Powdered graphite was used in one instance to pack the tube. It proved easy to reduce the porosity locally with the graphite and it appeared that packing with graphite would be an effective way to make the porosity of the tube uniform. Further testing, however, showed that the tube wall had a very eccentric pressure-flow relationship. Although the flow was uniform over the wall at one pressure, it was far from uniform at another pressure. In some places the flow even decreased with increasing pressure drop across the wall. The graphite was evidently forming compressible plugs in the pores in the wall, which tightened with increasing pressure drops, but why the graphite powder did this and the Plexiglass did not is obscure. The pressure drop from one end of the tube to the other was far less than that across the wall of the tube, so that the longitudinal pressure gradient in the tube had no appreciable effect.

The Flow System

A flow diagram for the experimental apparatus is shown in Figure 14. All the plumbing was hung on the wall, and the porous tube assembly was supported independently on a table and connected to the piping with rubber hose. The primary and secondary flows were measured with Fischer and Porter Flow-Rators, which were calibrated against critical flow orifaces before they were installed. The readings of the flow meters made during runs were corrected for pressure and temperature. The several flow meters were necessary to accomodate the range of flow rates while measuring always with reasonable accuracy. The accuracy of the flow measurements was 2% or better.

The structural features of the assembly of the porous tube and manifold are shown in Figure 15. The plastic tubes which form the entrance and exit sections screwed into plastic end plates. The end plates were drawn together by two steel rods so that they clamped the porous tube between them. The rods also took up the thrust against the end plates when the manifold was under pressure. A seal between the porous tube and the end plates was made by compressing an "O" ring into the joint. The holes where the steel bars passed through the end plates were adequately sealed by squeezing stopcock lubricant into them. The cylindrical outer shell of the manifold was sealed to the end plates with other "O" ring joints. The construction was very convenient, for the outer case could be removed without disturbing anything, making the interior parts easily accessible for work.

The secondary air supply was brought into the manifold through a rubber hose attached to the outer case, but the electrical connections were brought in through ports in the end plates so that they would not interfere with the removal of the case. The ports for the power leads were just rubber stoppers with a copper bar passing through them.

A single port for 20 thermocouple leads was made from a piece of soft rubber as shown in Figure 16. The leads were brought out through a slot in the rubber and then bent through individual cuts in the rubber. The rubber was then compressed into a recess in the end plate by screwing down a pressure plate over it.

All joints of the system were checked individually for leaks with a soap solution, and the system as a whole was checked by sealing off the outlet and inlet after filling the system with air to a pressure of several pounds per square inch. The rate at which the pressure declined showed that leaks were quite insignificant compared to the operating

flow rates. One deficiency in the checks deserves note. It was not possible to make a static pressure check of the seal between the porous tube and the end plates. A leak through this seal would not permit air to escape from the system, but would permit air to move from the manifold to the main tube by a path other than through the porous wall. The "O" ring seal is, however, a very reliable one especially when, as was true here, the pressure on the "O" ring was maintained not only by a positive mechanical force from the squeeze ring but also by the pressure difference across the seal itself.

The Electrical System

Figure 17 shows the electrical system schematically. The heater for the secondary air supply was a 2 ohm resistor mounted in a piece of plastic tube which was connected into the supply line of the secondary air. Electrical leads were brought out through the wall of the tube and sealed with Duco cement. The power input to the resistor was controlled by a variable transformer. The voltmeter measuring the potential across the resistor was used for a general guide in adjusting the power to the heater, and was not an essential part of the apparatus.

The porous tube was heated by passing an electrical current through it. It was important for this method of heating that the tube should be made of stainless steel which has one of the highest electrical resistivities of the metals. If the tube were made of a material with a lower resistivity, excessively heavy conductors would have been required to carry the current to the tube. As it was, the tube had a resistance of about .01 ohms and the current ranged up to about 70 amperes. The high current circuits were carried on 1 inch copper braid except in passing through the port into the manifold, where round copper bars were used. The braid was connected to the tube by separating its

strands to form a hole through which the tube could slip. The strands were then tightened over the tube at a point near its end where its oxide coating had been polished away. The connection was also painted with a conductive silver paint, but it is doubtful how much the paint contributed to the connection. The connections had low resistances as was demonstrated by the fact that there was no significant voltage drop across them with current passing through the tube, nor did the connections become hot.

The only other critical connection was between the copper bar passing into the manifold and the braid leading to the tube. This was a copper-to-copper connection which could be soldered in a straightforward manner. Connections outside the manifold required no special care since any heat dissipated in them neither entered the system nor influenced the measurements.

The heating current for the tube was supplied by a voltage step down transformer controlled on the primary side by a variable transformer as shown in Figure 17. The electrical input to the tube was measured both with a voltmeter and a ammeter connected through a metering transformer. The ammeter, which was calibrated against laboratory standard instruments, was the more accurate instrument and was relied on for the power dissipated in the tube wall. The voltmeter was used mostly to check that nothing had gone amiss in the connections to the tube that might cause a high resistance.

Temperature Measurements

Thirty gage copper-constantan thermocouples were used for all temperature measurements.

The wall temperature was measured by thermocouples set into little wells drilled part way through the wall. The leads adjacent to the couples were tied to the tube to place them along an isothermal and minimize heat flow along the leads. It made no difference in the thermocouple readings whether it was just resting in the well or was cemented into the well. Neither did the depth of the well make any difference. This indifferance to the method of connecting to the wall was taken as evidence that the thermocouple was in good thermal contact with the tube wall in all cases and was at the temperature of the wall. If the thermocouples had not been in good thermal contact with the wall, their reading would have changed as the contact was made better or worse in the different arrangements.

The temperature of the wall was measured at three different distances from the inlet to the porous tube. Measurements at the upstream station, about 3 diameters from the start of the porous tube, showed a higher heat transfer rate at that point in accordance with expectations, and this is undoubtedly due to the transient at the start of the heated section. Measurements at stations 11 and 14 diameters from the entrance did not differ significantly showing that the transient effects were no longer important. The measurements 3 diameters from the entrance were not recorded.

Although measurements on the same thermocouple were closely reproduceable, there was an appreciable variation among temperature measurements at equivalent points of the tube. This variation was probably due to the residual variation in the porosity of the tube. Variation in the heat dissipation may also have contributed. Measurements were, however, taken at three equivalent points 14 diameters from

from the entrance, and two equivalent points 11 diameters from the entrance, providing mean values more representative than any one reading and also making it possible to estimate the error in the mean. For most of the runs the standard deviation of the mean was about 5 percent of the mean.

The temperature of the air in the plenum chamber was measured with thermocouples placed in the manifold near the place where the wall temperature was measured. The thermocouples were enclosed in jackets of aluminum foil to put them in better contact with the air and reduce their thermal coupling to other objects by radiation. In spite of this precaution they were still influenced by the temperature of the porous tube, because of the relatively poor heat transfer between the thermocouple and the slowly moving air in the plenum chamber. In all cases, however, the temperature of the wall and the air in the plenum chamber was adjusted to be the same before data was recorded for computation. The thermocouples in the air gave adequate indications of the equality of the air and wall temperatures.

The temperature of the primary air inlet was measured with a thermocouple shielded in a length of hypodermic tubing. The tubing pointed into the air stream so that there was air circulation past the thermocouple junction and out through several small holes drilled in the needle. The inlet temperature was measured about 10 diameters upstream of the porous tube. Since the temperature of the gas in the inlet stream was ambient, there could be no changes in temperature across the tube or between the point of measurement and the porous tube.

The temperature of the air issuing from the tube was measured with a similarly assembled thermcouple at a point about 15 diameters downstream from the porous tube. It was the bulk or mixed mean

temperature that was desired from this thermocouple, and to promote mixing, an orifice restricting the tube to about 3/4 diameter was put in the stream at the outlet of the porous tube, and a screen was put in the stream 5 diameters down from the porous tube. As a result, there was no discernible temperature difference across the tube at the point of measurement.

The leads from the thermocouples were brought to a switch which permitted any thermocouple to be connected into the measuring circuit. The measurements of the thermocouple emf's were made with a Leeds and Northrup K-2 potentiometer and a galvanometer. The over-all sensitivity of the apparatus was about .5 microvolts. Since absolute temperature measurements were not needed, the thermocouple in the inlet air stream was used as the reference.

The thermocouple leads which entered the switch were connected to brass elements which formed the actual switching contacts. In effect, this produced an additional pair of junctions in the circuit which also contributed to the emf measured by the potentiometer. To nullify the effects of the switch junctions, the switch was designed to be at uniform temperature. The whole switch assembly was mounted on a heavy aluminum plate and the thermocouple leads were strapped to this plate for 2 inches before entering the switch housing to insure that no junction would be heated or cooled by the leads. The housing of the switch was shielded with aluminum foil making contact with the mounting plate except for a small area where the switch handle protruded. The handle was insulated from the switching mechanism by a plastic link to reduce heat conduction to the junctions from the operator's hand.

There were other junctions in the thermocouple circuit in the potentiometer and the galvanometer, but they were all between copper,

declines as exp $(-Vx/\alpha)$, where V is the velocity of the approaching fluid, x is distance from the wall, and α is the thermal diffusivity of the fluid. For the experiments here (V/α) is of the order .1 cm, so that heat conduction dies out very fast.

To reduce heat loss by radiation, a cylinder of aluminum foil was placed about a half inch from the tube. The foil had holes punched in it to permit air to pass through to the porous tube. On the inside of the tube radiation was not a problem because the transparent gas did not interact with the radiative flux from the tube.

The dimensions and thermal conductivity of the tube were such that negligible heat was conducted longitudinally in the wall.

As a check on the effectiveness of the control of the heat flow, energy balances were made in some preliminary runs. In these runs the secondary gas stream was not heated to the temperature of the tube wall so that they offer if anything a more severe test of heat losses from the tube. The enthalpy difference between the entering and effluent gas streams within 3 percent of the electrical power applied to the tube and varied both above and below the electrical input. The variation is only slightly more than the sensitivity of the flow meters and gives strong evidence that there were no significant heat leaks.

Taking Data and Calculations

The procedure in taking data and making calculations was to set the flow rates in the streams to give approximately the desired values of Reynolds modulus and the parameter V/U_b. The heating circuit controls were next adjusted so that the temperature of the porous tube was the same as that of the secondary air stream. After a few minutes readings were made and recorded for the flow meters, manometers, heating

brass, and manganin, which have very low thermoelectric power against each other and did not need the precautions taken for the brass-constantan junctions in the switch.

As a check on the suppression of all spurious emf's, a second thermocouple was installed in the inlet stream (in addition to the reference thermocouple) which could be switched into the place of the operating thermocouples. With this thermocouple in the circuit a measurement of the total spurious emf could be made, and it was never observed to be more than 1 microvolt.

For the small range of temperatures over which the apparatus was used the emf of the copper-constantan junction could be assumed to be a linear function of the temperature, and, in accordance with the calibration specified for the thermocouple materials, the thermoelectric power of the junction was taken as 41 volts per degree C.

Control of Heat Leaks

A difficult and important part of any quantitative experimentation with heat transfer is insuring that the heat flows where it is supposed to flow and there only. The critical heat flow in the experiments described here was that which was conducted from the porous tube to the gas stream in its interior, and the control of this heat flow was an important consideration in the design of the experiments. In the first place, the generation of the heat in the wall of the tube eliminated any possibility of losses in ducts. The air outside the tube was adjusted to be the same temperature as the tube so that heat would not be conducted away from the tube in an outward direction. Furthermore, if there was any small mismatch of the temperature of tube and air, the heat transferred was minimized by the flow of gas towards the tube wall which swept the heat back to the wall. More precisely, the heat flux

declines as exp $(-Vx/\alpha)$, where V is the velocity of the approaching fluid, x is distance from the wall, and α is the thermal diffusivity of the fluid. For the experiments here (V/α) is of the order .1 cm, so that heat conduction dies out very fast.

To reduce heat loss by radiation, a cylinder of aluminum foil was placed about a half inch from the tube. The foil had holes punched in it to permit air to pass through to the porous tube. On the inside of the tube radiation was not a problem because the transparent gas did not interact with the radiative flux from the tube.

The dimensions and thermal conductivity of the tube were such that negligible heat was conducted longitudinally in the wall.

As a check on the effectiveness of the control of the heat flow, energy balances were made in some preliminary runs. In these runs the secondary gas stream was not heated to the temperature of the tube wall so that they offer if anything a more severe test of heat losses from the tube. The enthalpy difference between the entering and effluent gas streams was within 3 percent of the electrical power applied to the tube and varied both above and below the electrical input. The variation is only slightly more than the sensitivity of the flow meters and gives strong evidence that there were no significant heat leaks.

Taking Data and Calculations

The procedure in taking data and making calculations was to set the flow rates in the streams to give approximately the desired values of Reynolds modulus and the parameter V/U_b. The heating circuit controls were next adjusted so that the temperature of the porous tube was the same as that of the secondary air stream. After a few minutes

readings were made and recorded for the flow meters, manometers, heating current for the porous tube, and all the thermocouples. After the thermocouple potentials had been recorded, the flow meters were checked to insure that they had not drifted from their earlier values.

The measurements were recorded on data sheets, and the computations were continued on the same sheets to avoid any transcribing. The reading of each flow meter was interpreted with a calibration plot and then corrected for density differences from the conditions of the calibration to give the flow rates in the streams. From these, velocity through the wall and the bulk velocities and Reynolds numbers at the several points of the tube could be calculated. The power and the power per unit area of the wall can be calculated from the current in the tube. The thermocouple readings at equivalent points (all those at the same distance from the entrance) were averaged to give the temperature of the tube wall. The temperature of the secondary stream and the bulk temperature at each station were obtained from an energy balance over the appropriate part of the tube.

An ambiguity arises in the computation of q if the temperature of the tube is not exactly the same as that of the secondary air stream, for it is not clear how much heat exchange there is within the wall. In such cases, two values of q were set down, one assuming that no heat was transferred within the wall, and the other assuming that the gas came to equilibrium within the wall. The truth certainly lies somewhere in between. In most of the cases the difference between the two values of q is not large and the average value was taken for the calculation of the Nusselt modulus. At higher flow rates, however, mismatches of

the temperatures produce a relatively greater range of ambiguity in q. From these cases, a series of runs were made with the same conditions of flow throughout but changing the electrical current in the tube. Values of Nusselt modulus based on the two assumptions about q were plotted against the power dissipated in the tube. The two values of Nusselt modulus became identical when the temperature of the tube equalled that of the gas passing through the wall, and this common value was taken as its true value. The plots also showed that the average value of q, which was used in the less critical cases, was a good approximation.

APPENDIX IV

THE EXPERIMENTAL DATA

The essentials of the experimental data are tabulated on the next page so they will be available for anyone who wishes to apply a different interpretation to them. An explanation of the several columns follows. All temperatures are relative to that of the fluid entering the porous tube.

Sta	Station 1 on the tube, 36.5 cm from entrance Station 2 on the tube, 27.8 cm from entrance
Re	Reynolds modulus at point of measurement $2aU_b/\nu$
V_w/U_b	Ratio of velocity of fluid passing through wall to bulk velocity of fluid flowing in tube
t_w	Temperature of wall in °C. (Average from 2 or 3 thermocouple readings.)
t_3	Temperature of outlet stream in °C
t_m	Mixed mean temperature of fluid in tube at point of measurement in °C
P/A	Power dissipated in wall of tube (watts/cm^2)
Nu	Nusselt modulus. $Nu = (2a/k)q/t_w - t_m$. As described in Appendix III, q was taken as $P/A + 1/2\ V_w C(t_p - t_w)$ where t_p is the temperature of the fluid in the plenum chamber.

The constants used in the calculations were

C -	volumetric heat capacity	.00118 joules/cm^2 - °C
k -	thermal conductivity	.000263 watts/cm - °C
a -	radius of tube	1.27 cm
ν -	kinematic viscosity	.161 strokes

Sta	Re	V_w/U_b	t_3	t_w	t_m	P/A	Nu
1	49,900	0	1.30	7.12	1.23	.0763	125
2	49,900	0	1.30	6.46	.90	.0763	132
1	50,800	.0004	1.44	7.19	1.35	.0760	127
2	50,500	.0004	1.44	6.59	1.04	.0760	132
1	51,400	.0009	1.634	7.54	1.52	.0763	122
2	50,800	.0009	1.634	6.89	1.17	.0763	128
1	51,500	.0016	3.22	12.59	2.98	.1097	115
2	50,400	.0017	3.22	11.71	2.26	.1097	119
1	30,000	0	1.68	8.10	1.59	.0595	88
2	30,000	0	1.68	7.95	1.17	.0595	85
1	30,000	0	1.68	8.10	1.59	.0595	88
2	30,000	0	1.68	7.95	1.17	.0595	85
1	30,300	.0004	1.34	6.37	1.25	.0424	80
2	30,100	.0004	1.34	5.94	.96	.0424	83
1	30,100	.0009	1.68	7.24	1.56	.0442	76
2	29,700	.0010	1.68	6.80	1.20	.0442	78
1	30,100	.0040	2.54	6.64	2.35	.0288	68
1	30,700	.0025	2.20	7.20	2.03	.0398	73
1	30,100	.0040	4.07	11.06	3.77	.0524	66
2	28,400	.0043	4.07	10.56	2.98	.0524	66
1	30,200	.0039	3.73	9.86	3.44	.0436	69
1	30,100	.0040	2.50	6.50	2.31	.0274	68
2	28,400	.0043	2.50	6.18	1.82	.0274	68
1	29,700	.0053	2.88	6.46	2.67	.0239	64
1	14,800	.0055	2.48	5.89	2.30	.0168	45
1	15,400	0	0	11.37	2.49	.0496	54
2	15,400	0	0	11.26	1.89	.0496	51
1	14,800	.0023	3.15	9.93	2.92	.0282	40
2	14,300	.0023	3.15	9.3	2.8	.0282	42
1	14,100	.0011	1.63	6.16	1.51	.0203	44
2	13,900	.0011	1.63	5.90	1.17	.0203	44
1	14,500	.0016	2.22	7.62	2.06	.0235	42
2	14,200	.0016	2.22	7.19	1.59	.0235	42
1	14,800	.0023	2.92	9.38	2.70	.0276	40
2	14,300	.0023	2.92	8.80	2.10	.0276	41
1	14,900	.0032	3.34	9.55	3.10	.0276	40
2	14,200	.0034	3.34	8.89	2.44	.0276	42
1	47,700	.0123	1.40	5.25	1.32	.0472	(1)
1	47,700	.0123	.99	3.85	.94	.0281	(1)
1	47,700	.0123	1.51	6.44	1.41	.0588	(1)

Sta	Re	V_w/U_b	t_3	t_w	t_m	P/A	Nu
1	48,900	.0023	1.59	5.30	1.46	.0411	(2)
1	48,900	.0023	1.96	6.90	1.82	.0608	(2)
1	50,000	.0032	2.05	6.60	1.90	.0579	(3)
1	50,000	.0032	1.58	4.37	1.45	.0270	(3)
1	50,000	.0032	1.83	5.39	1.69	.0411	(3)

(1) This group of measurements was plotted against P/A as described in Appendix III to give Nu = 111.

(2) This group of measurements was plotted against P/A as described in Appendix III to give Nu = 111.

(3) This group of measurements was plotted against P/A as described in Appendix III to give Nu = 111.

APPENDIX V

LITERATURE REFERENCES

1. J. E. Broadwell, P. Sherman, Survey of Porous-Wall Heat-Transfer Literature, Engineering Research Institute, Contract AF18(600)-51, April, 1953.

2. S. Goldstein, Modern Developments in Fluid Dynamics, Oxford University Press, 1938.

3. S. W. Yuan, A. Finkelstein, Laminar Flow with Injection and Suction Through a Porous Wall, presented at Heat Transfer and Fluid Mechanics Institute, 1955.

4. J. Laufer, The Structure of Turbulence in Fully Developed Pipe Flow, NACA TN 2954, 1953.

5. T. von Karman, The Analogy Between Fluid Friction and Heat Transfer, Trans. ASME, 61:705, November, 1939.

6. S. Weinbaum, H. L. Wheeler, Heat Transfer in Sweat-Cooled Porous Metals, Jour. Appl. Phys. 20-1, 113-122, Jan., 1949.

7. H. L. Weissberg, A. S. Berman, Velocity and Pressure Distributions in Turbulent Pipe Flow with Uniform Wall Suction, presented at Heat Transfer and Fluid Mechanics Institute, 1955.

8. R. G. Deissler, Analytical and Experimental Investigation of Adiabatic Turbulent Flow in Smooth Tubes, NACA TN 2138, 1950.

9. J. H. Clarke, R. H. Menkes, P. A. Libby, A Provisional Analysis of Turbulent Boundary Layers with Injection, Jour. Aero. Sci., 22:255, April, 1955.

10. H. S. Mickley, R. C. Ross, A. L. Squires, W. E. Stewart, Heat, Mass, and Momentum Transfer for Flow Over a Flat Plate with Blowing or Suction, NACA TN 3208, July, 1954.

11. W. H. Dorrance, F. J. Dore, The Effect of Mass Transfer on the Compressible Turbulent Boundary Layer Skin Friction and Heat Transfer, Jour. Aero. Sci., 21:404, July, 1954.

12. J. Nikwiadse, Forschungsheft 356 des Vereins Deutscher Ingenieure, 1932.

FIGURES

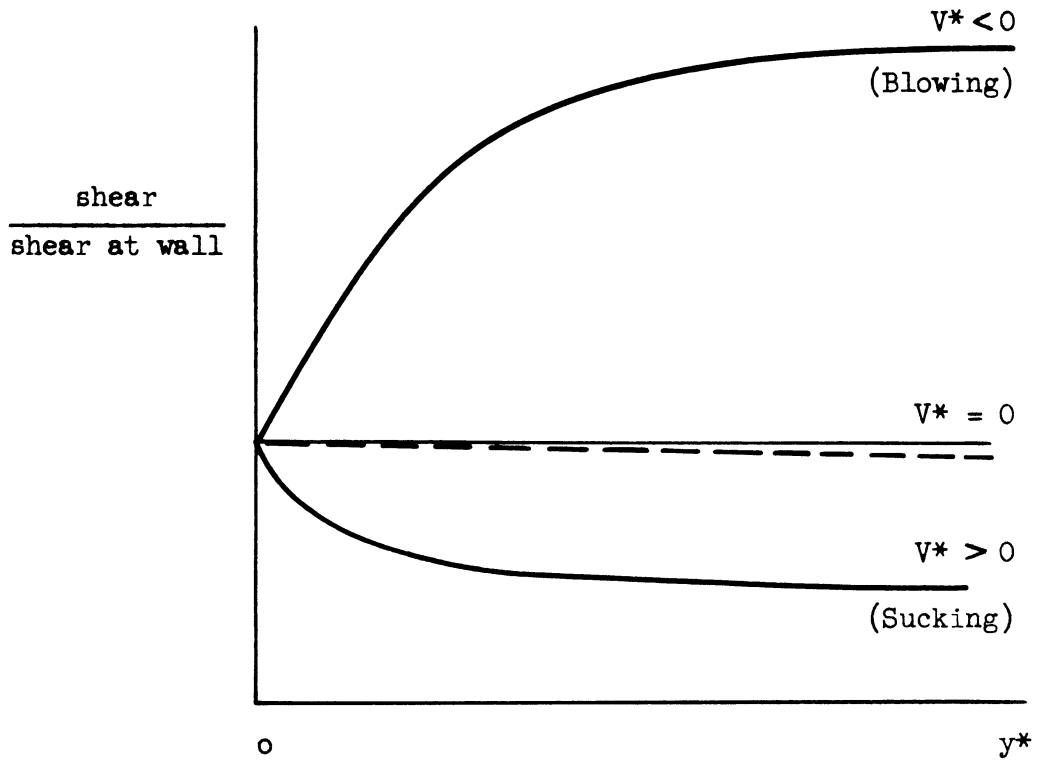

--- is without assumption r/a = 1

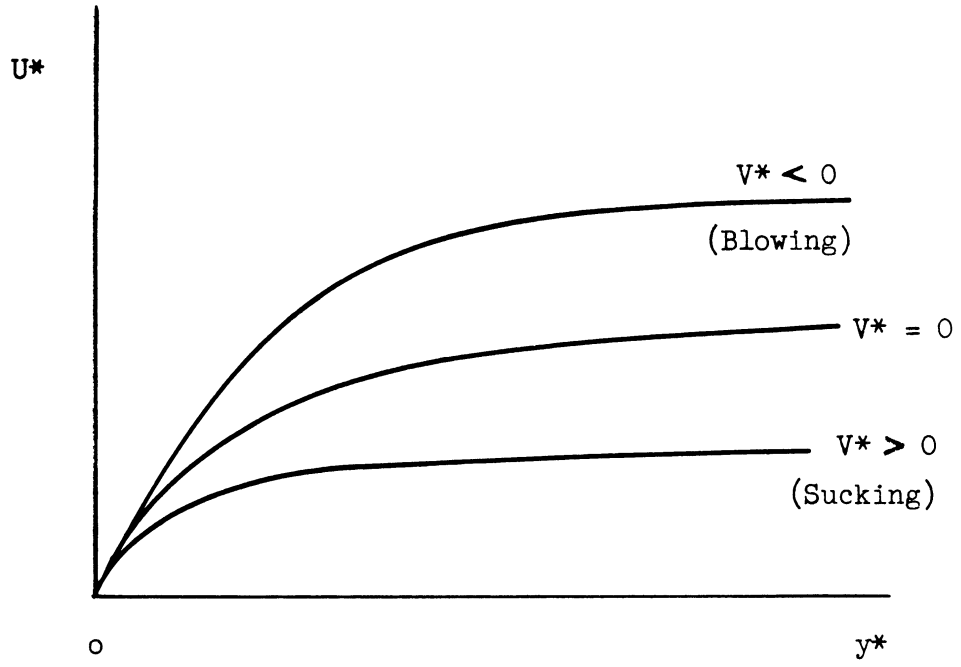

Figure 1 Effect of Flow Through Wall on Shear

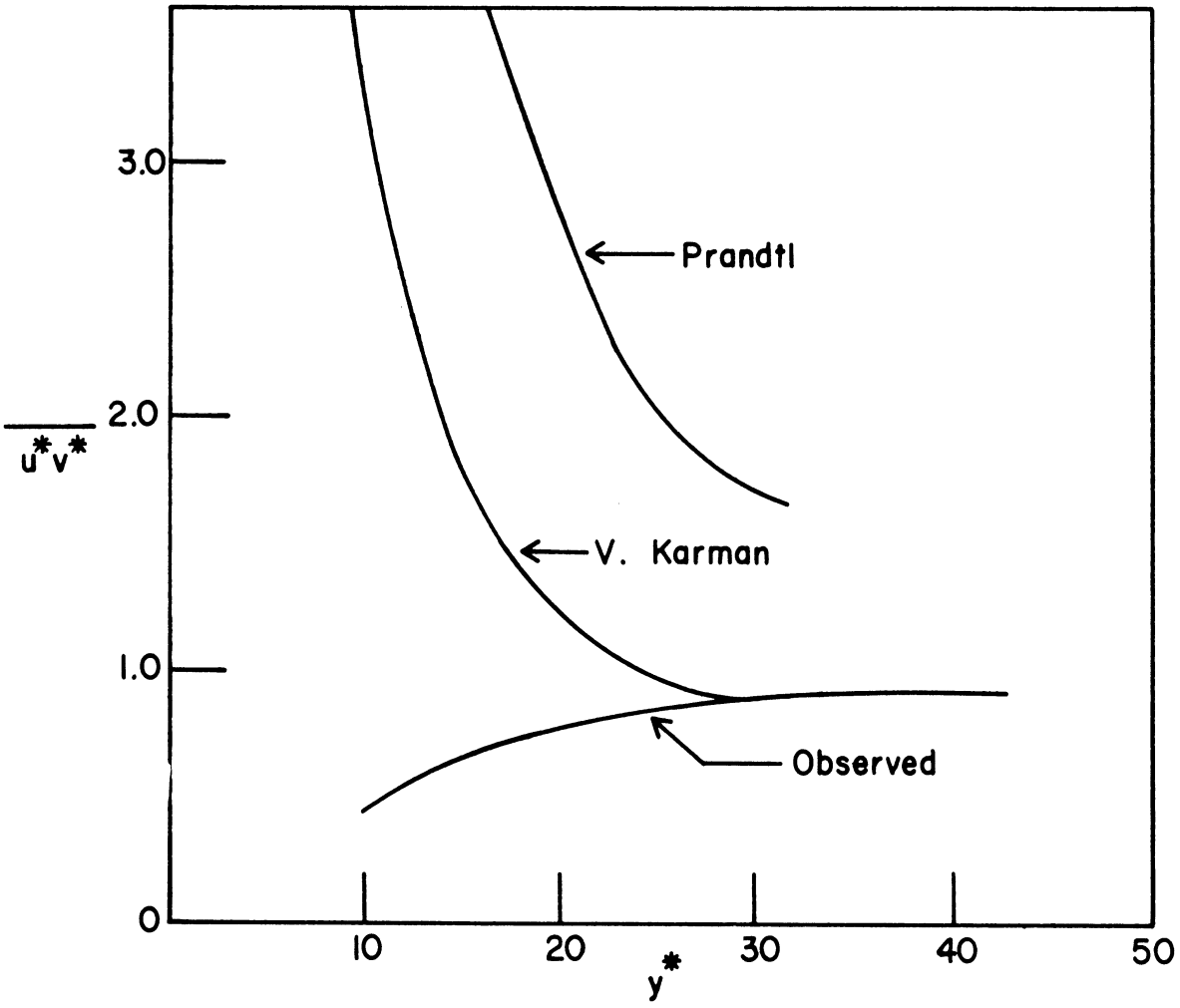

Figure 2 Comparison of Expressions for Turbulence

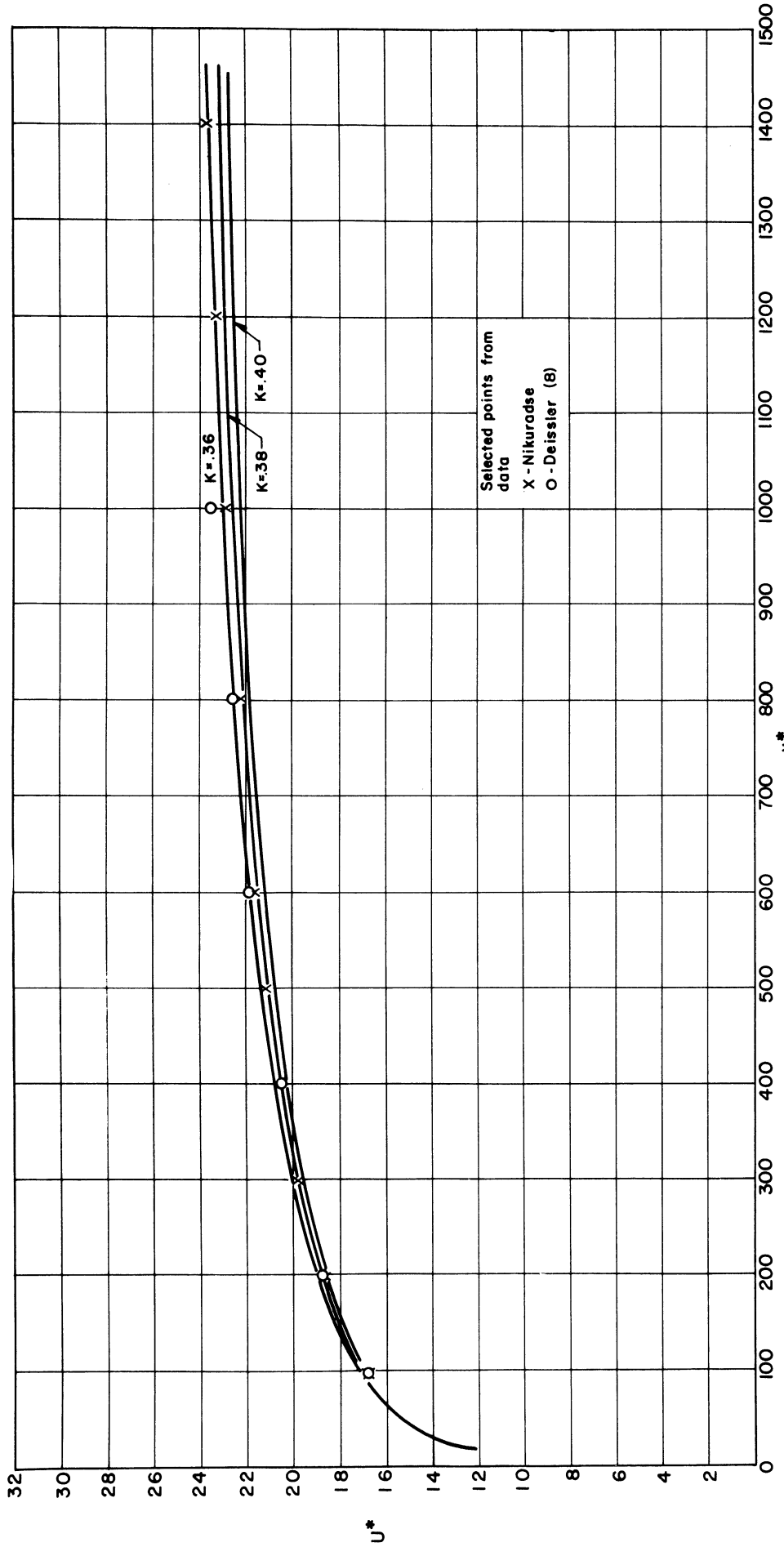

Figure 3 Effect of Constant K on Velocity Profile

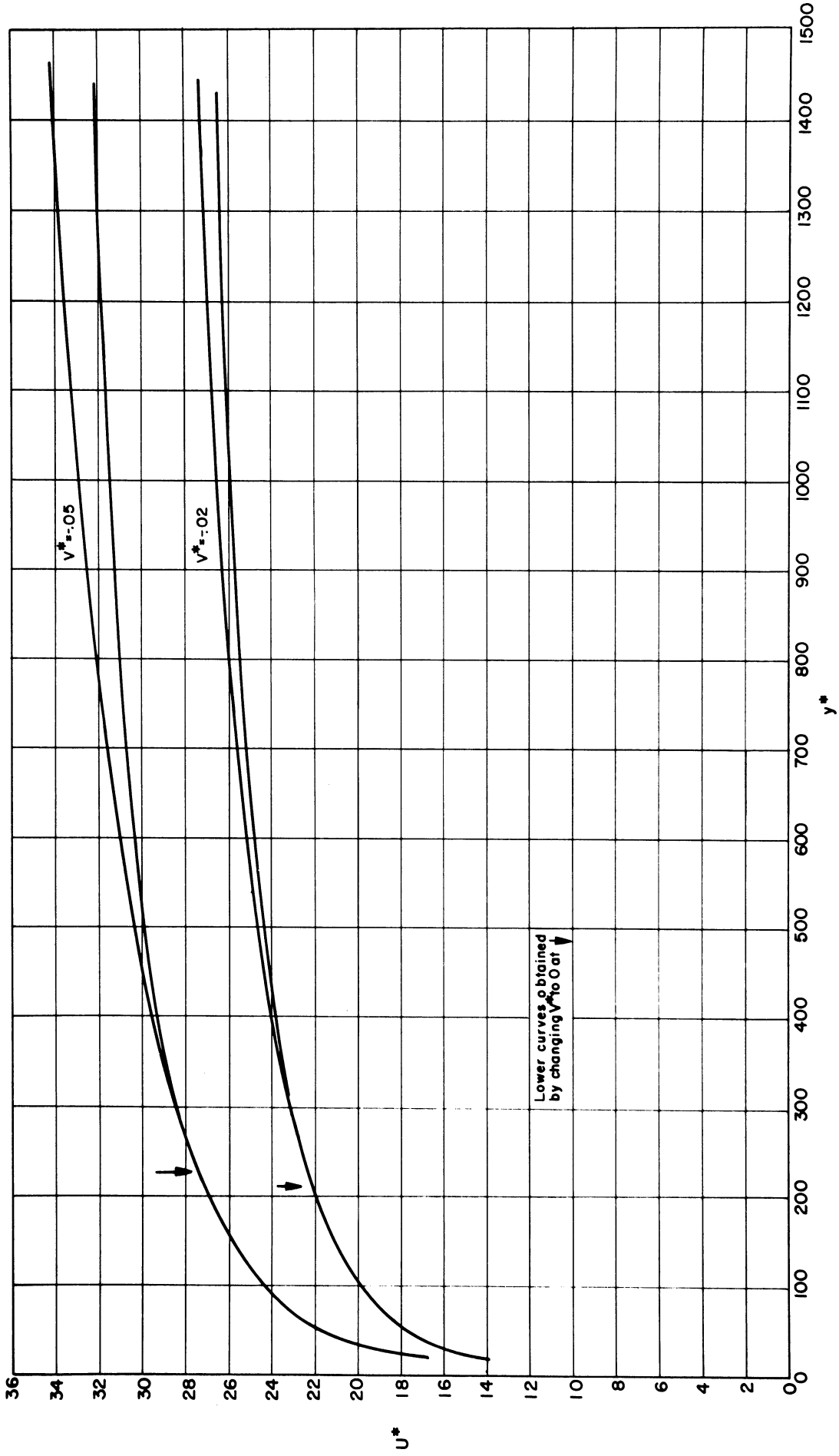

Figure 4 Effect of Radial Variation of V on Velocity Profile

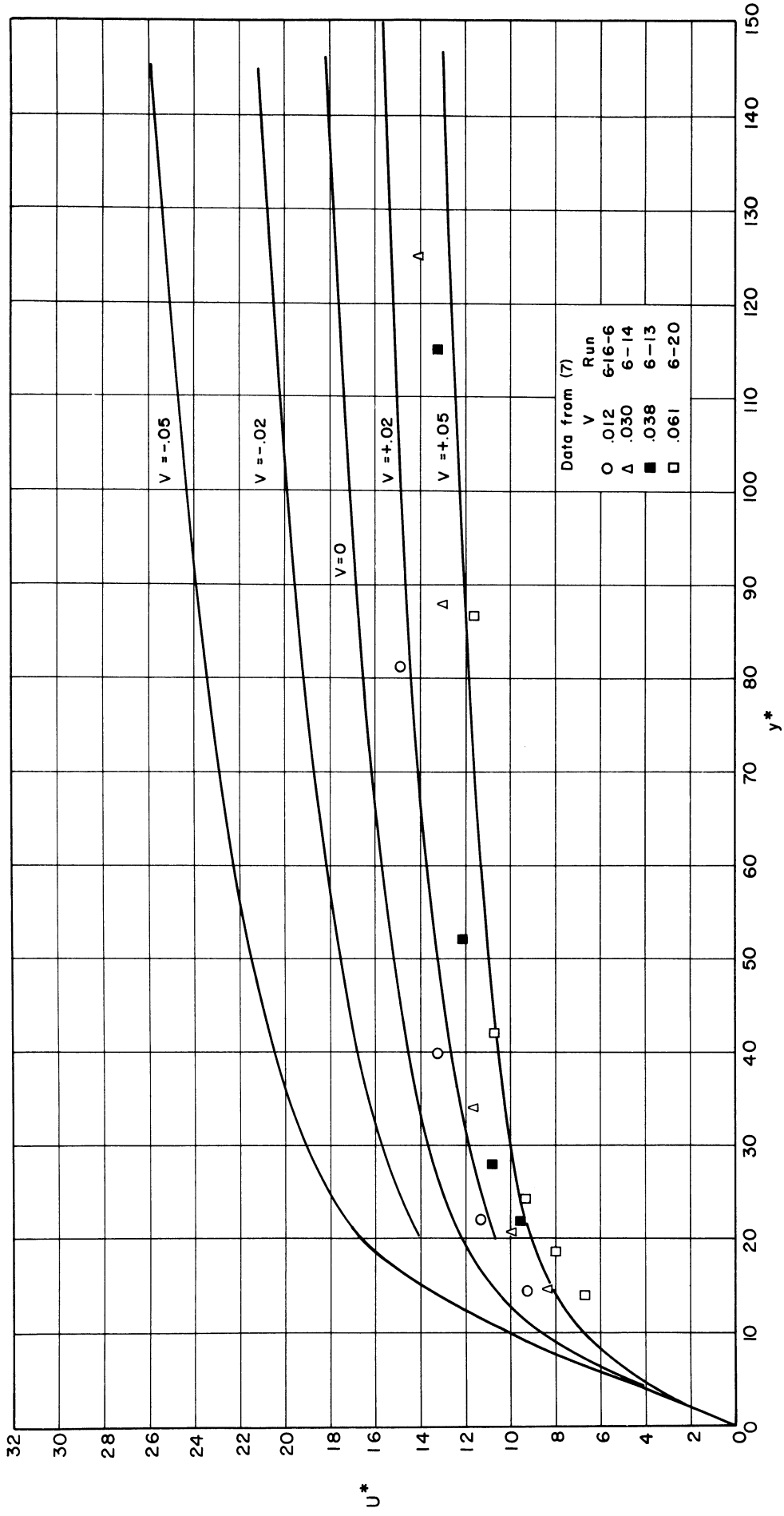

Figure 5 Velocity or Temperature Profile

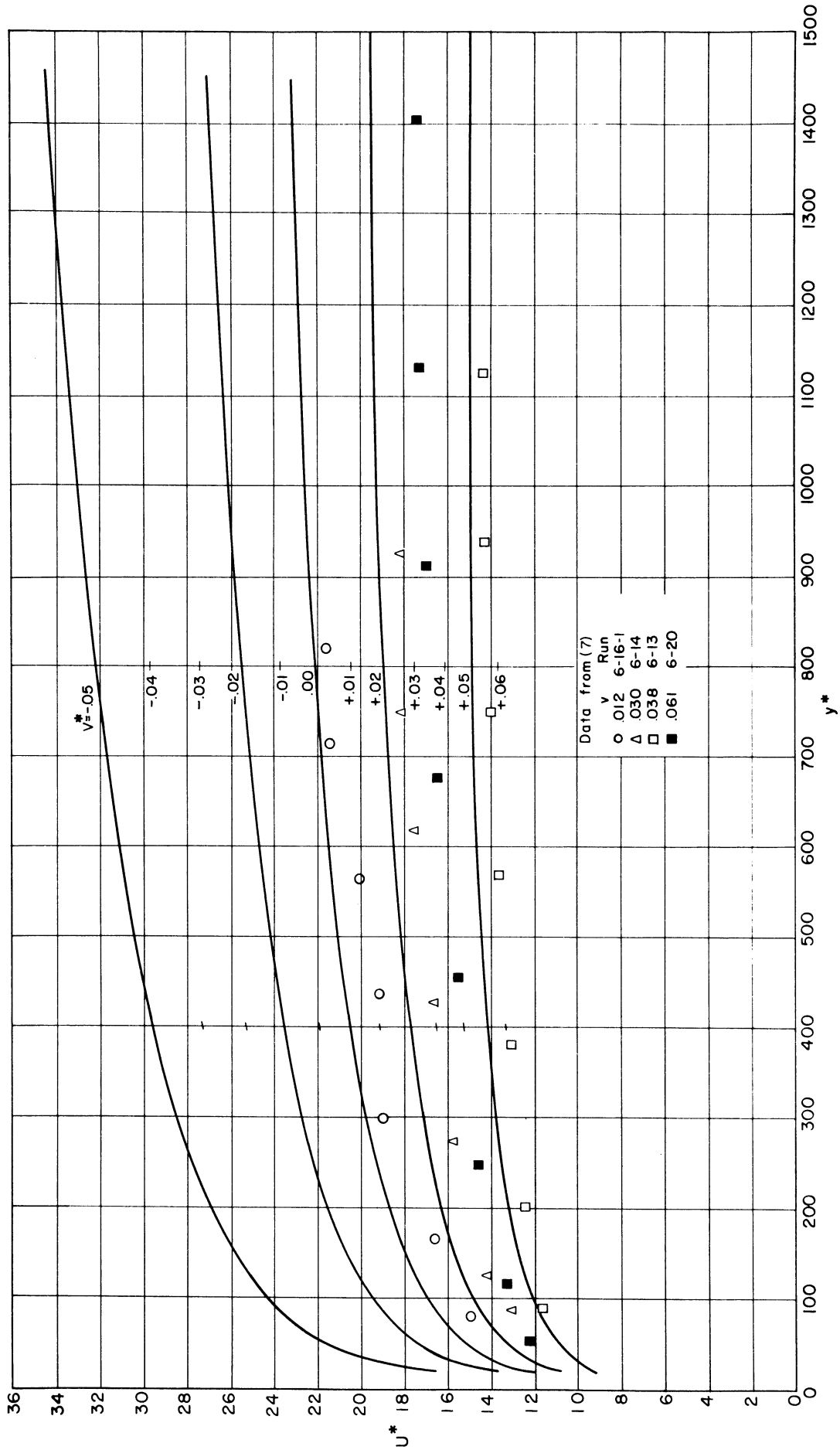

Figure 6 Velocity or Temperature Profile

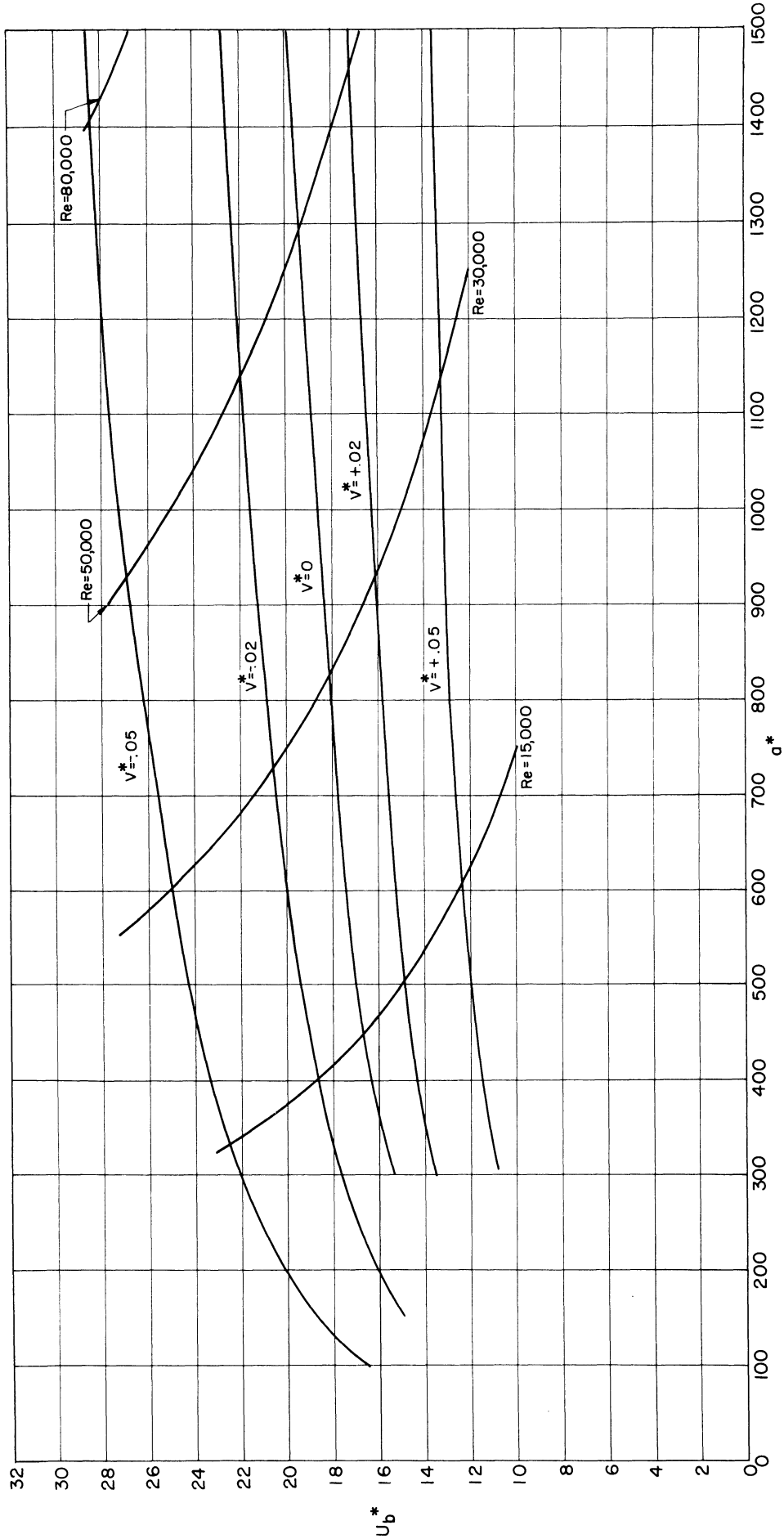

Figure 7 Bulk Velocity

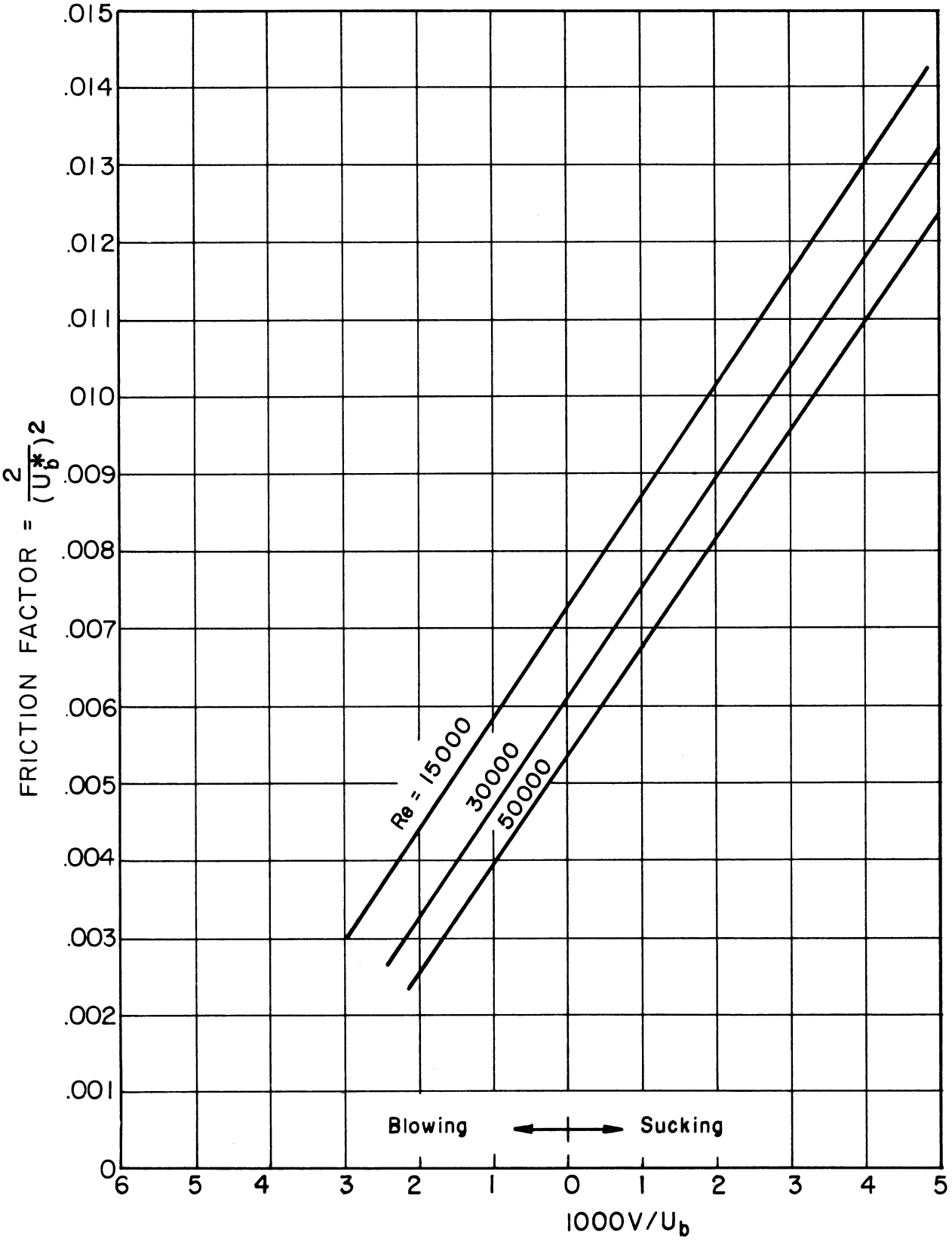

Figure 8 Prediction of Friction Factor

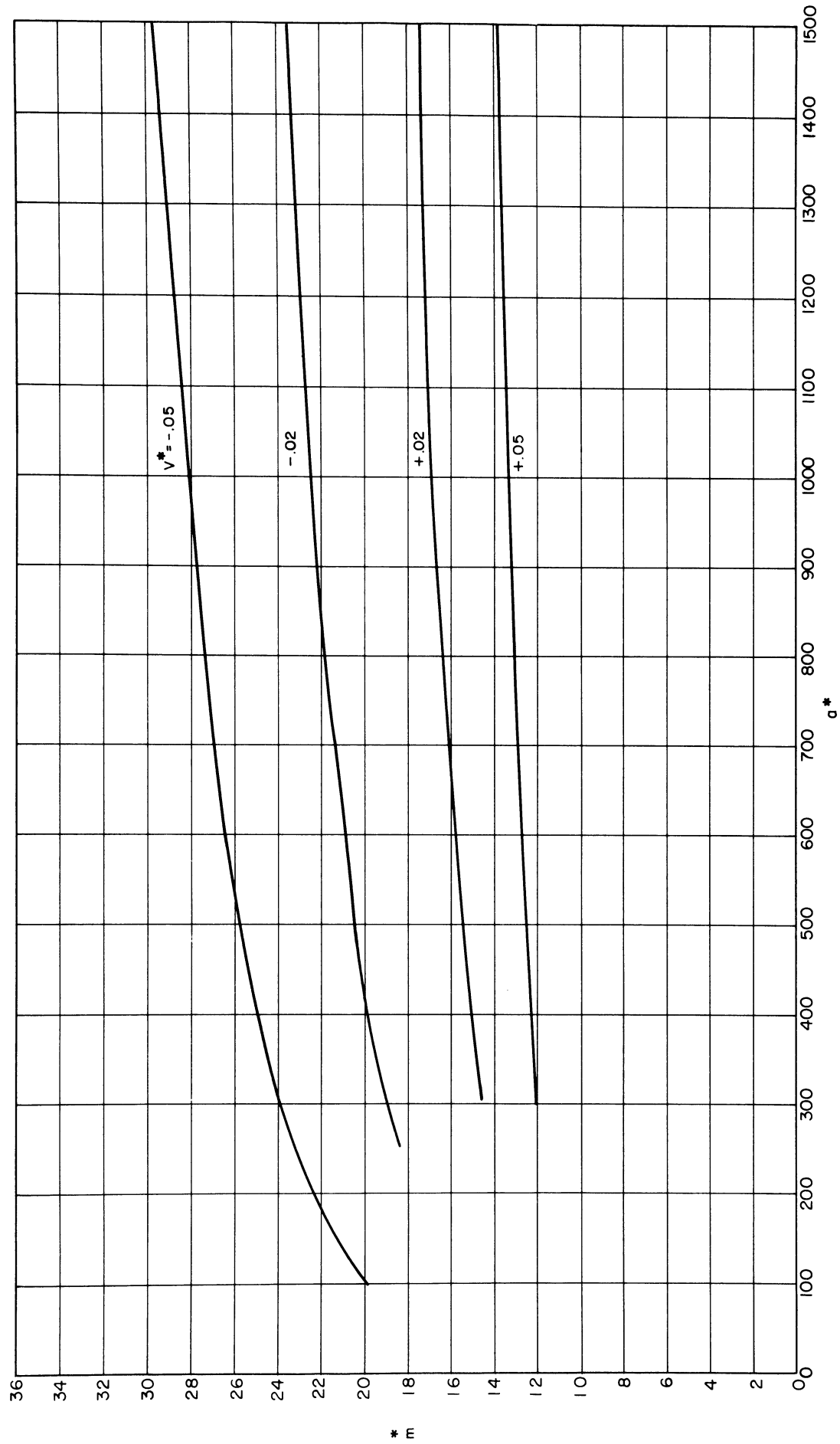

Figure 9 Mean Temperature of Stream

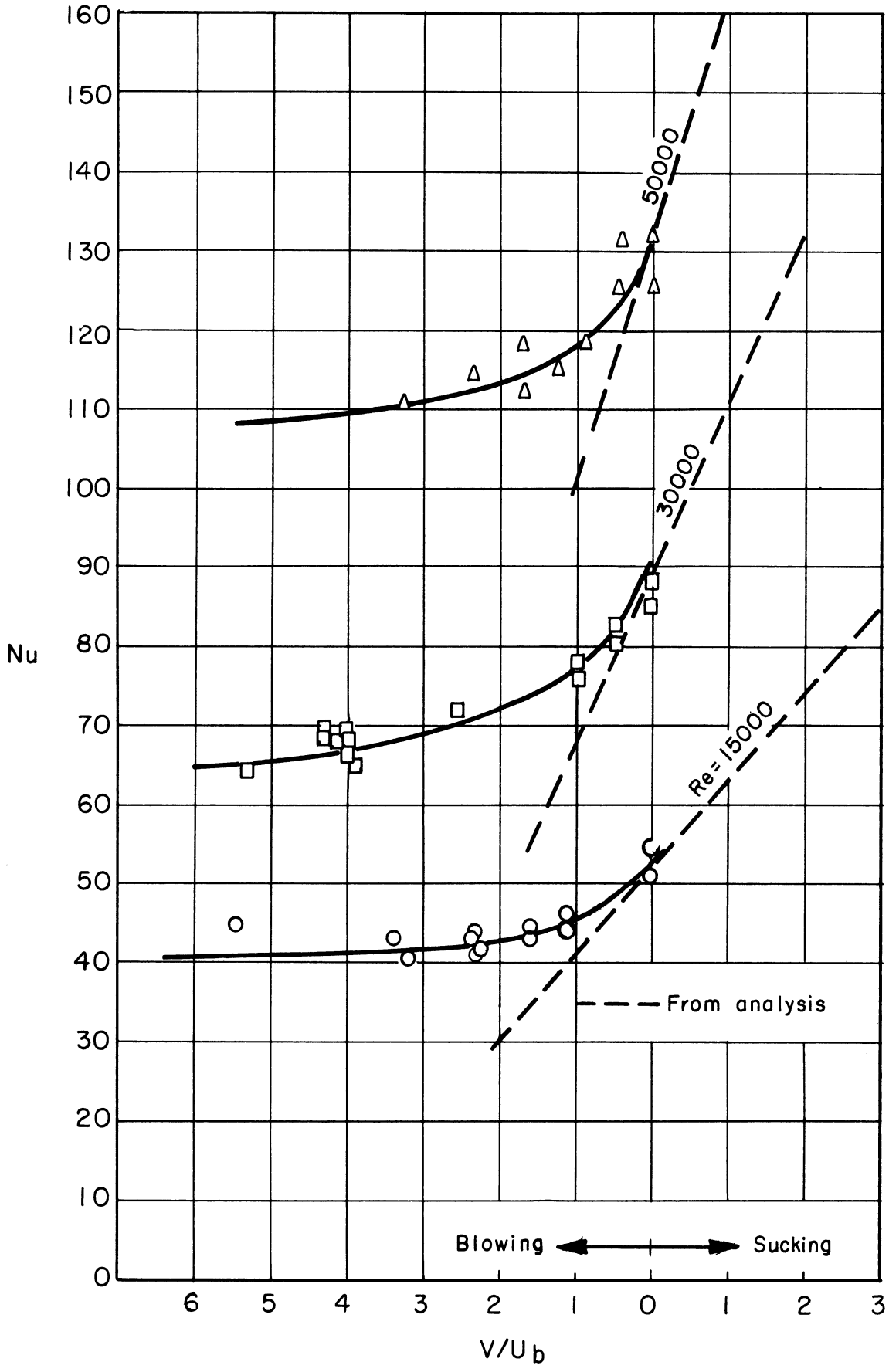

Figure 10 Predicted and Measured Nusselt Modulus

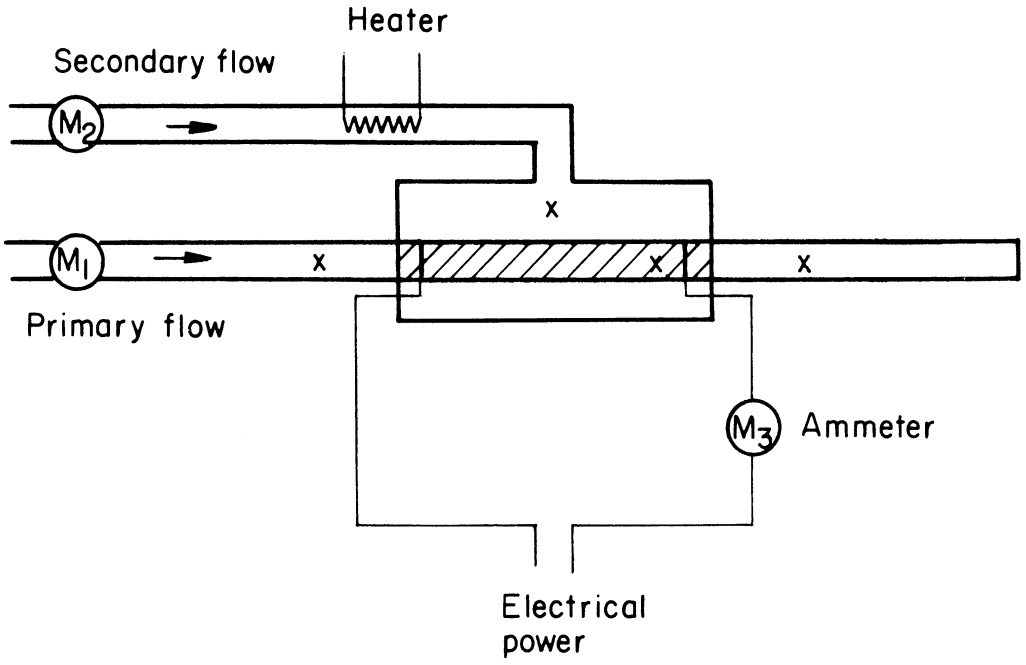

x indicates point of temperature measurement

Figure 11 Simplified Diagram of Apparatus

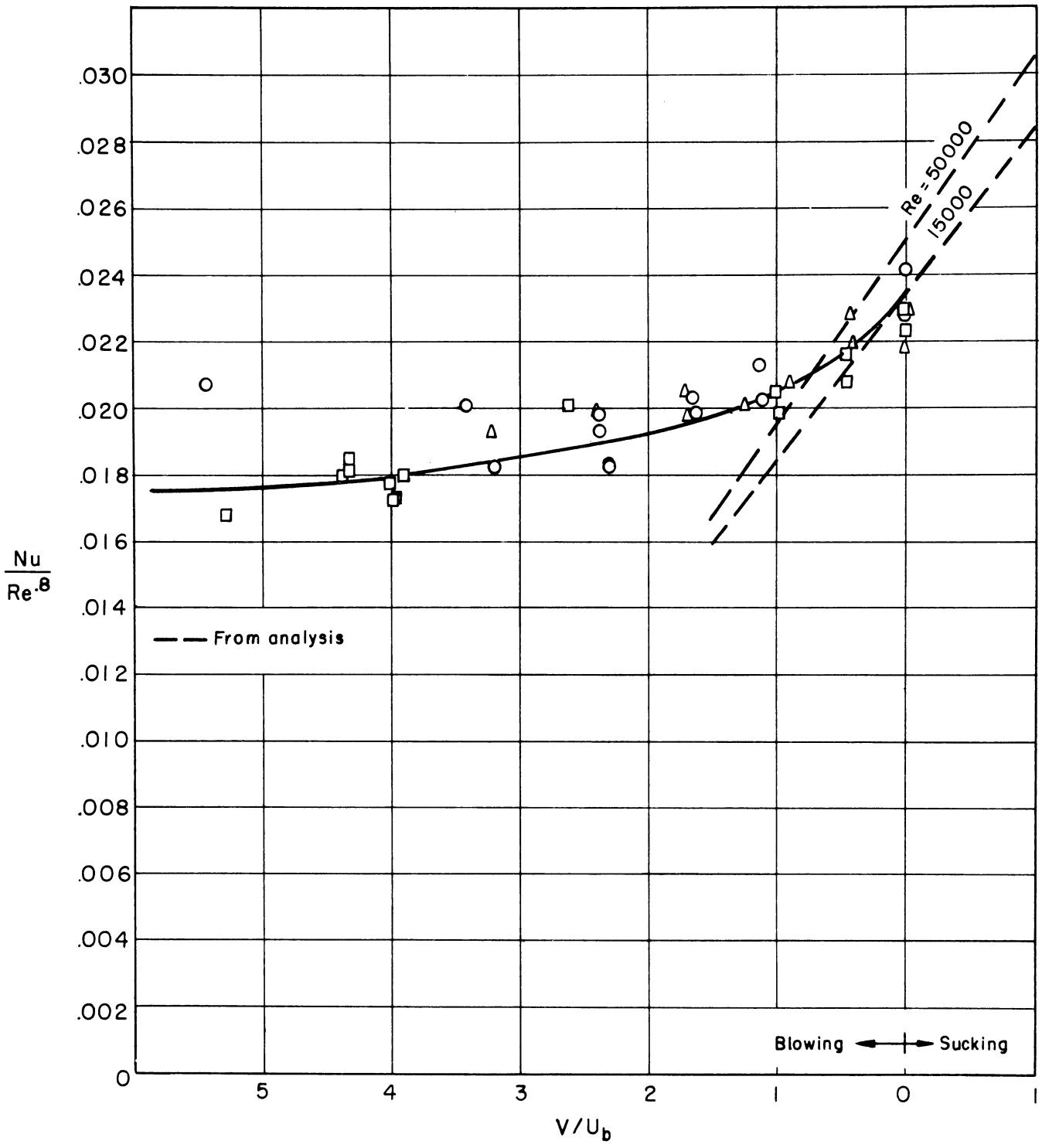

Figure 12 Correlation of Data

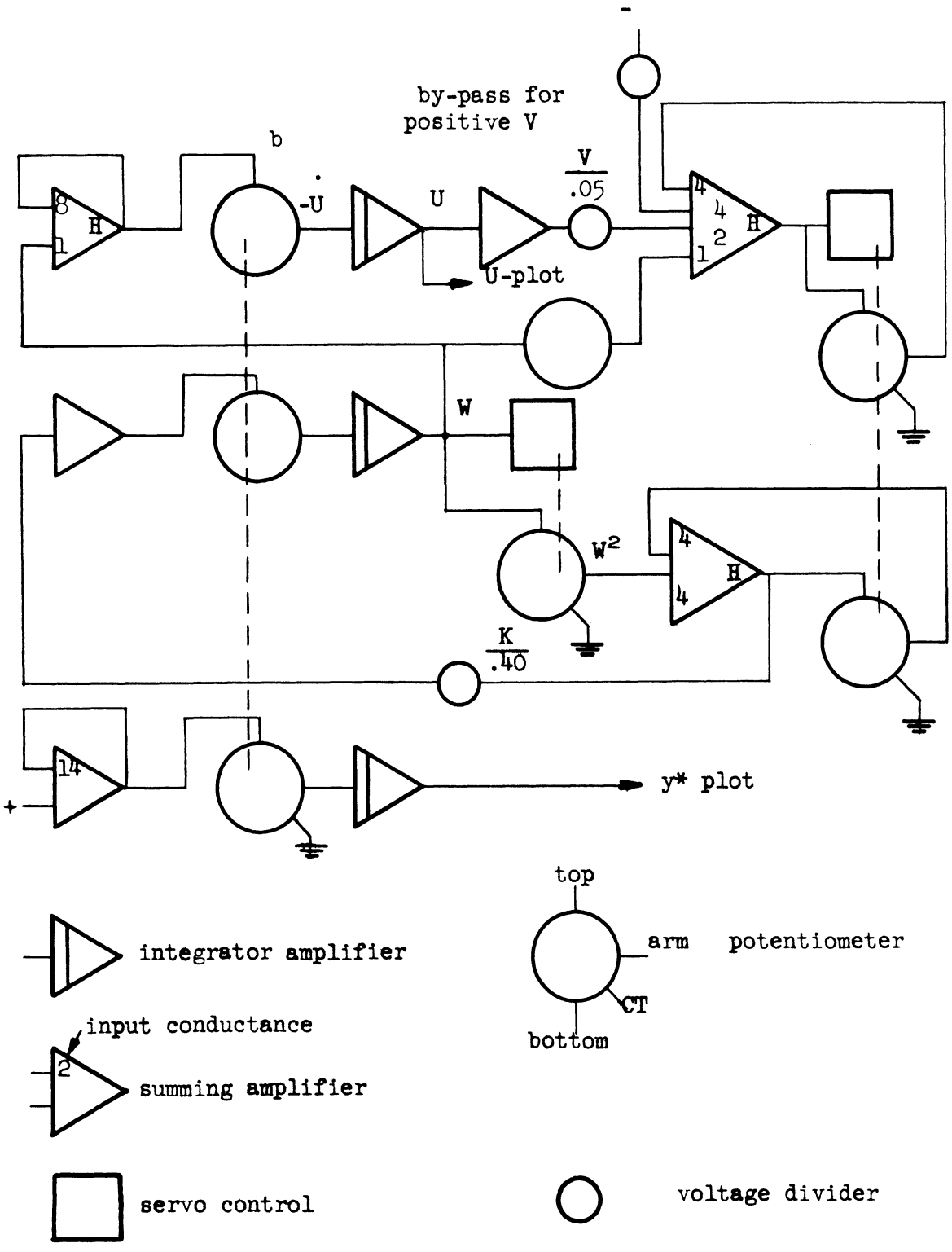

1. Input conductances are 1 unless otherwise noted.
2. All summing amplifiers have a feedback conductance of 1 that is not shown unless marked with an H.

Figure 13 Differential Analyzer Circuits

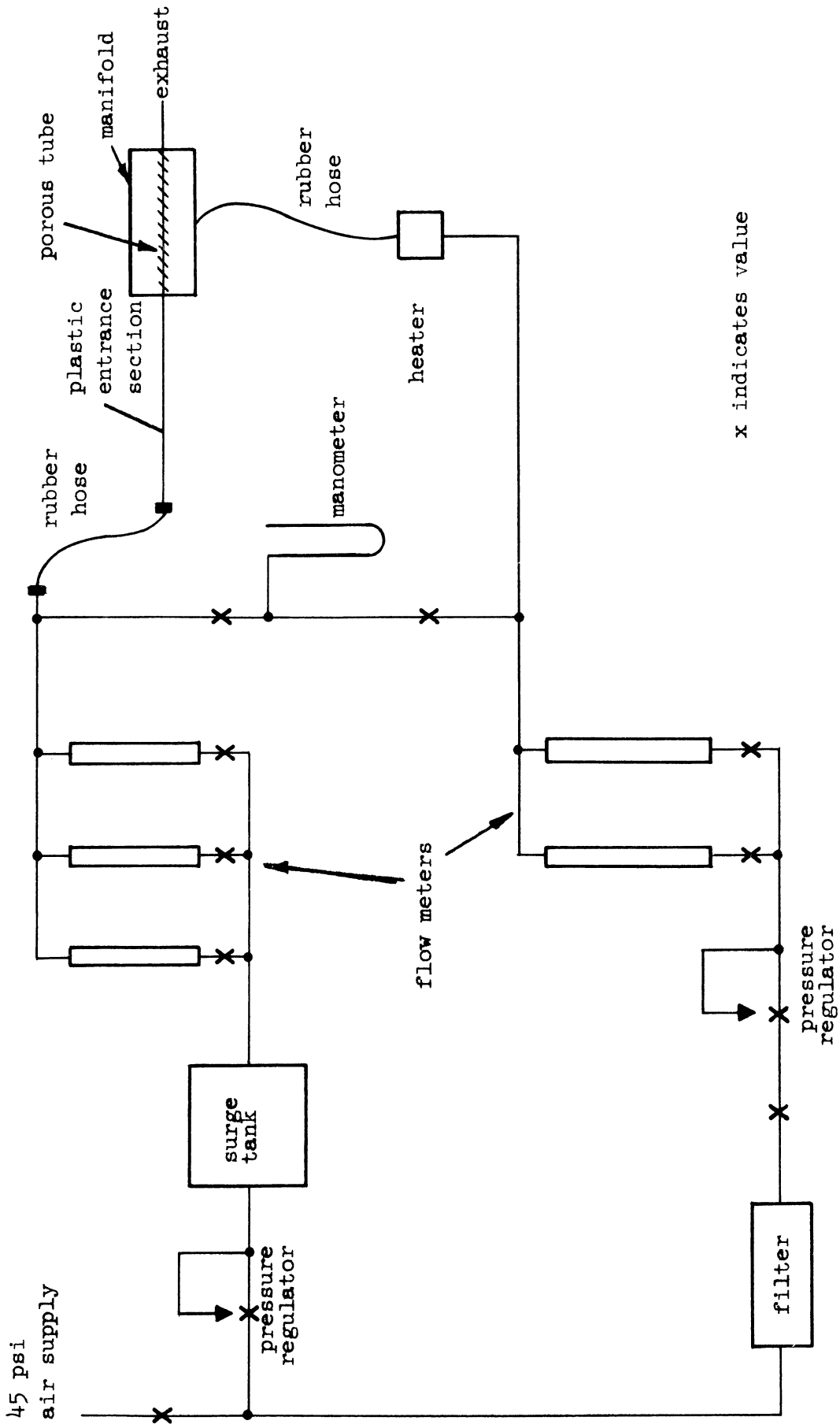

Figure 14 Flow Diagram

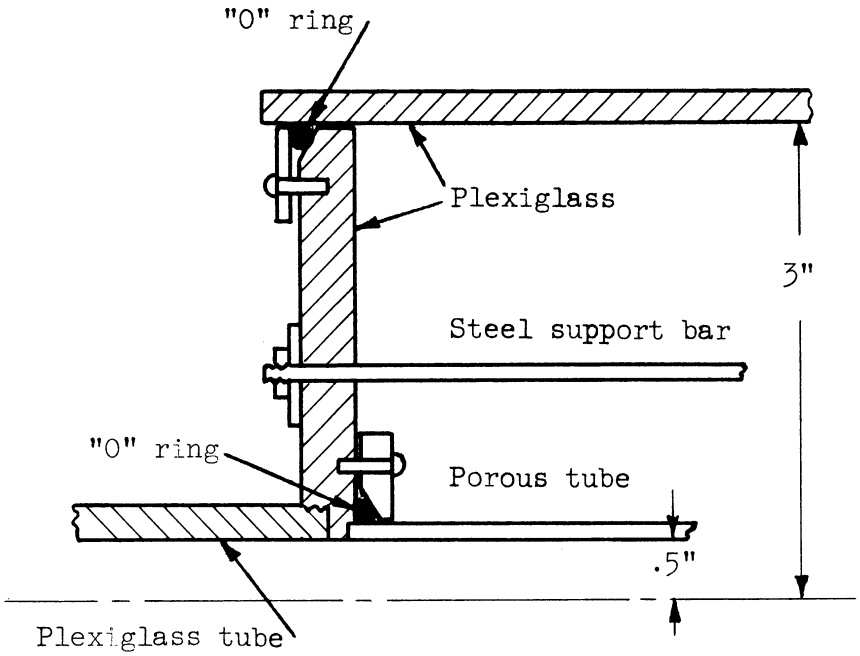

Figure 15 Details of Construction

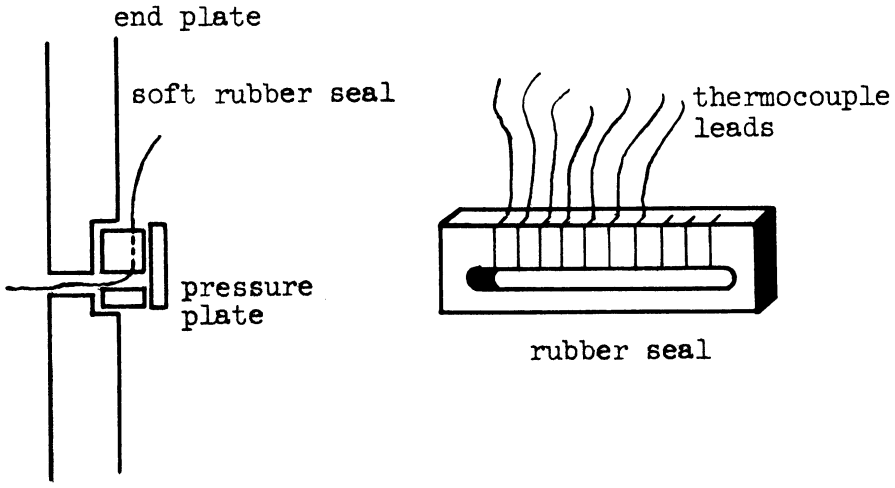

Figure 16 Port for Thermocouple Leads

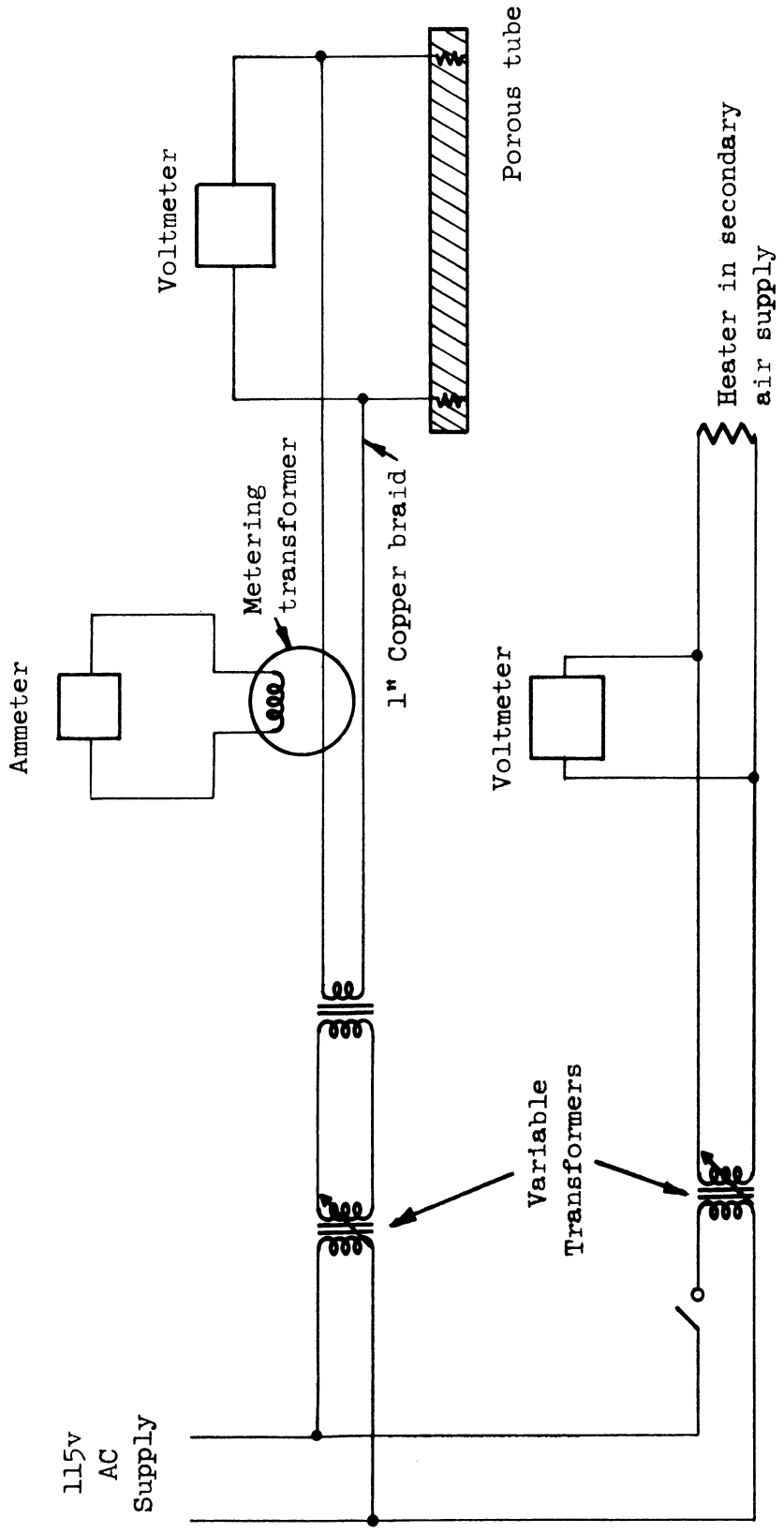

Figure 17 Electrical Heating Circuits